Macromolecules

pubs.acs.org/Macromolecules

Article

Structural Design of CANs with Fine-Tunable Relaxation Properties: A Theoretical Framework Based on Network Structure and Kinetics Modeling

Osman Konuray, Xavier Fernández-Francos,* and Xavier Ramis

Cite This: *Macromolecules* 2023, 56, 4855−4873

Read Online

ACCESS | Metrics & More | Article Recommendations | Supporting Information

ABSTRACT: In this work, we present a model capable of reproducing the stress relaxation dynamics of a wide range of relaxation processes in covalent adaptable networks (CANs) produced by stepwise polymerization. The proposed model captures the effective elastic response of the material subject to an initial stress by analogy with a network decrosslinking process. The combination of a recursive structural model and a kinetic model for the bond exchange reaction makes it possible to predict the expected stress relaxation profile in simple and complex systems depending on the structure of the network, the rate of bond exchange of the different components, and the presence of permanent bonds. After the basic features of the model are analyzed, its prediction capabilities are validated by simulating a number of scenarios taken from the literature. The results show that tailoring of the network architecture enables unprecedented flexibility in the design of CAN-based materials.

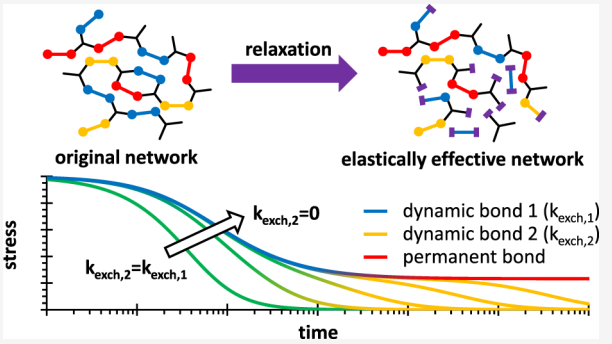

INTRODUCTION

Reversible covalent chemistry has recently found widespread application in polymer networks, enabling useful material properties such as healability and recyclability.[1−5] More and more dynamic bond exchange reactions are being discovered that allow materials to adapt to environmental stimuli, without losing their network integrity. From the limited set of reactions that were used 10−15 years ago, the broad selection of reactions available today makes it possible to design materials for a wide range of applications and processing scenarios.

Research efforts are also being directed to the study of the structural and kinetic effects of dynamic bond exchange processes via analysis of stress relaxation and creep experiments. A number of interesting results have been reported in the literature, based on (a) the tailoring of the network architecture by introducing a controlled amount of permanent bonds (i.e., bonds incapable of dynamic exchange), (b) the combination of different bond exchange reactions or mechanisms, (c) the use of dynamic monomers with different bond exchange kinetics, or (d) the modification of the crosslinking density by changing the functionality of the crosslinkers.

Li et al.[6] studied the effect of introducing permanent bonds in the network structure of thiol-epoxy vitrimers with the purpose of controlling creep. A theoretical threshold for the limiting ratio of permanent bonds was defined, based on the concept of a permanent network structure. Breuillac et al. described networks with dual dynamic and static crosslinks based on dioxaborolane chemistry.[7] They found that the concentration of crosslinking units plays a relevant role in the relaxation kinetics, and that the combination of static and dynamic crosslinks helped control creep, and the materials retained good adhesion capabilities. In a recent work by our group, the correlation between network permanency and covalent adaptation in a thiol−ene polymer was studied using a theoretical model based on structural fragments. The extent of relaxation of strain-induced stress was accurately predicted as a function of the dynamic bond content. Moreover, it was shown that the materials maintained their recyclability up to a limiting fraction of permanent crosslinks.

Complex systems involving more than one relaxation mechanism have also been investigated. Van Lijsebetten et al. reported vitrimeric materials consisting of components that follow a similar dissociative bond exchange mechanism but with different kinetics.[8] The authors developed a model based on the combination of different Maxwell relaxation elements in order to explain the complex relaxation behavior of the materials. Xiang and Zhou designed interlocked CANs based on the combination of dynamic exchange processes that are

Received: March 15, 2023
Revised: May 17, 2023
Published: June 23, 2023

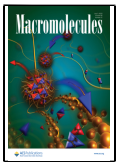

activated upon exposure to different stimuli.[9] Wang et al. prepared dual-crosslinked materials with superior creep resistance by combining boronic ester crosslinks with physical H-bonding that limit chain segment diffusion.[10] Later, an original strategy was reported by Van Lijsebetten for the control of the undesired creep of low T_g vinylogous urethane vitrimers, based on the release of blocked amines by high temperature reversible cyclization of dicarboxamide structures.[11] Alternatively, Konuray et al. combined two bond exchange reactions with distinct kinetics and obtained a material that relaxes stresses in a sequential manner.[12] Similarly, El-Zaatari et al. studied the effect of the intrinsic bond exchange kinetics of different crosslinkers on the relaxation behavior of crosslinked polydimethylsiloxane and showed that combinations of different crosslinkers led to intermediate relaxation behavior.[13] In slight contrast, Porath et al. produced polysiloxane vitrimers with boronic ester crosslinks having distinct bond exchange dynamics, wherein mixed materials generally showed relaxation behavior closer to the faster dynamic component.[14]

Interesting effects depending on the network structure have also been reported. Isogai and Hayashi observed a significant effect of the crosslinker functionality on the relaxation by transesterification of thiol-epoxy networks, similar to what other researchers have reported.[15] Melchor Bañales and Larsen showed that the activation energy of guanidine metathesis in crosslinked networks differed significantly from that of model compounds due to mobility limitations.[16] Hajj et al. observed that the relaxation kinetics of polyimine vitrimers was accelerated when the crosslinking density decreased.[17] Zhao and Abu-Omar designed transesterification-based vitrimers with tunable relaxation kinetics by reducing the crosslinking density and increasing the concentration of available hydroxyl groups.[18] Hayashi and Yano studied the effect of crosslinking density of transesterification vitrimers without changing the total concentration of hydroxyl groups but did not observe any positive effect on the relaxation kinetics.[19] Moreover, Chen et al. showed that increasing the crosslinking density without changing the functionality of the crosslinking agent decreased the relaxation time in polyester vitrimers.[20] Hu et al. combined different concurrent bond exchange reactions in vitrimers and showed that the molecular structure significantly impacted the relaxation kinetics.[21] Wu et al. related the relaxation dynamics to the degree of crosslinking of vitrimers based on dioxaborolane metathesis.[22,23] Interestingly, a faster exchange rate was reported between dangling chains and crosslinks than between crosslinks themselves, evidencing a strong influence of the network structure on the relaxation dynamics.[22]

In light of all these reports, one can argue that there are complex structural factors playing a role in the relaxation kinetics of vitrimeric materials. It is acknowledged that there are intrinsic reactivity effects that contribute to the reported results, such as the presence of hydroxyl groups in transesterification polyester vitrimers.[18−20] However, it is the authors' belief that there are certain structural effects that have not been properly taken into consideration. The results from Li et al.[6] and Konuray et al.[12] suggest that some relaxation effects can be analyzed from a structural point of view. Other works describing the effect of monomer functionality on the relaxation kinetics[15,17] point in a similar direction.

The stress relaxation of CANs based on dissociative bond exchange processes deserves some analysis. The classification of dissociative CANs as vitrimer or vitrimer-like materials is a matter of debate.[4,5,24,25] Despite harboring dissociative bond exchange processes, other CANs have been reported to exhibit stress relaxation processes similar to those exhibited by associative vitrimers.[8,24] As an example, Chakma et al. reported the relaxation behavior of dissociative networks based on anilinium salts and compared them with furan-maleimide Diels−Alder materials.[26] Interestingly, CANs based on anilinium salts showed very little temperature dependence of the equilibrium constant, leading to a modulus nearly constant with temperature, similar to associative vitrimers.[26] Jourdain et al. studied dissociative CANs based on triazolium crosslinks with distinct temperature-dependent equilibrium and used both vertical and horizontal shifts to build stress relaxation master curves.[27] Van Lijsebetten analyzed the relaxation kinetics of dissociative CANs based on transesterification of phthalate monoesters by considering the existence of complex exchange processes and estimated the extent of dissociation based on the equilibrium modulus at different temperatures.[8] The analysis of stress relaxation processes of CANs based on Diels−Alder showed that the dynamics were governed by the rate of the backward (dissociation) reaction.[28]

Network structure analysis has been already employed, to some extent, to analyze the properties and behavior of vitrimers and other CANs. The effect of the transesterification equilibrium on the network structure of epoxy-acid based vitrimers was modeled by Altuna et al. using a recursive methodology based on structural fragments.[29] This modeling methodology was used to analyze the proportion of covalently bonded tertiary amine catalyst in the gel and sol fractions of the material in order to understand the effect of the catalyst on its relaxation kinetics.[30] Strachota et al. used the theory of branching processes to analyze the effect of temperature on the network structure and thermal−mechanical properties of materials based on associative Diels−Alder bond exchange reactions.[31] This same methodology was later employed for the study of self-healing materials based on copolymers with permanent bonds and inter-penetrated network structures.[32] The well-known Flory−Stockmayer equation was employed in order to establish a criterion for the degelation threshold of Diels−Alder networks upon heating.[33−35] Van Lijsebetten et al. modeled the effect of dissociative exchange on the initial crosslinking density of materials undergoing stress relaxation.[8] Parada and Zhao analyzed the bond exchange dynamics starting from a preliminary structural analysis of ideal network structures, leading to a theoretical relaxation behavior that could be represented by a single Maxwell element.[36]

The present work proposes a further step toward the use of network structure models for the analysis of the dynamics of the stress relaxation processes in CANs and to analyze complex kinetic and structural effects observed in relaxation processes. A recursive method based on the definition of structural fragments and their connections[37−39] will be used. A number of relevant statistical averages will be defined in order to analyze the evolution of the elastically active network structure during bond exchange. To characterize the process, some relevant parameters based on key composition and functionality features of the network will also be defined. The concept of permanent polymer/network structure will be used to define characteristic maps for the analysis of stress relaxation capabilities of the materials.[6] A kinetic model will be defined and employed to relate the evolution of the network structure with the observed stress relaxation kinetics.

https://doi.org/10.1021/acs.macromol.3c00482
Macromolecules 2023, 56, 4855−4873

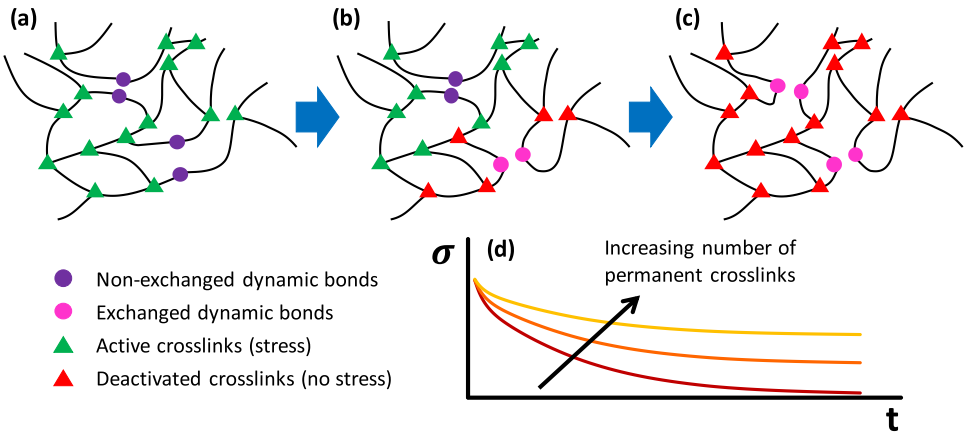

Figure 1. Schematics of a network relaxation process produced from the exchange of dynamic bonds: (a) initial stretched polymer network, (b) partially relaxed network, and (c) completely relaxed network. (d) Stress relaxation processes with varying contribution of permanent crosslinks.

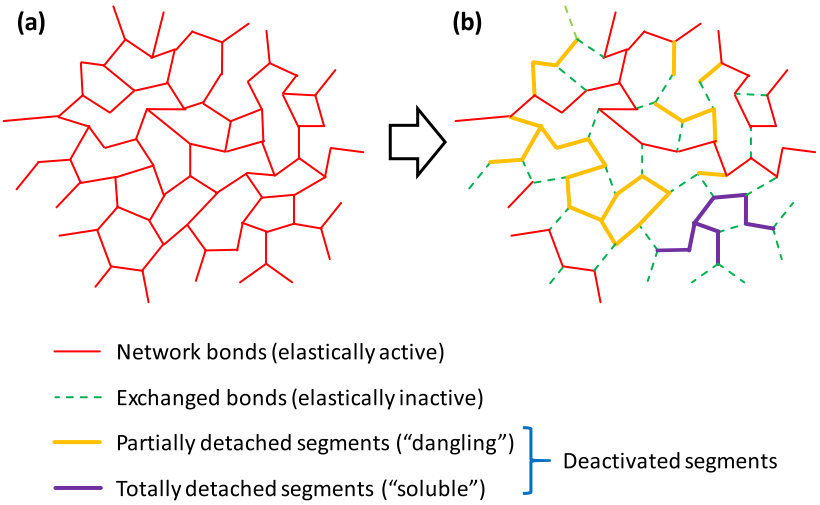

Figure 2. Effect of the bond exchange process on the effective network structure of a material during a stress relaxation experiment. (a) Initial material and (b) material with partial bond exchange.

After introducing the structural model and its key features, the effect of the composition of the network structure will be discussed in detail. This will be followed by the introduction of the kinetic model that will be used to analyze the kinetic effects and to model complex stress relaxation processes in CANs, including those with dissociative bond exchange. The effect of relaxation mechanisms with different kinetics will be considered in the model. The results and the trends predicted with the model will be discussed and compared with those published in the literature. A number of useful conclusions in terms of structural design of CANs will be drawn from this analysis.

THEORY

The analysis starts from the description of the phenomena taking place in a stress relaxation process of a given polymer network with dynamic bond exchange. First, a stretched polymer network, as shown in Figure 1a, is considered, in which the different crosslinks (green triangles) are active (i.e., all the network strands between crosslinks contribute to the stress response). The dynamic bonds undergoing exchange reactions, which in doing so change from purple to pink circles, as shown in Figure 1b, lead to the breaking of existing network strands (stretched and contributing to stress) and formation of new ones (relaxed/non-stretched and not contributing to stress). This results in the deactivation of crosslinks (green triangles turning into red triangles), thereby transforming elastically active network strands (EANS) into non-elastically active strands, facilitating the relaxation of the stress. Eventually, at some point, all the crosslinks are deactivated as in Figure 1c, leading to complete relaxation of the initial stress.

Bonds are being broken and formed continuously in the process, so that the number of total bonds in the network structure remains constant; this is true also for CANs with dissociative exchange mechanisms at constant temperature,[25] for which it is possible to observe relaxation processes[8,24,27] in a similar way to associative CANs. The process of deactivating the existing crosslinks, as shown in Figure 1, can be regarded as a decrosslinking process, since the effect of exchanging dynamic bonds produces a similar effect to that of a real cleavage of these bonds in terms of the stress response of the material. The equivalence of deactivating elastically active crosslinks to a decrosslinking process is illustrated in Figure 2. At the beginning of the process, the stretched material is made up of a crosslinked network containing a number of elastically active network chains (a) (red bonds) which produce a stress response when stretched. Upon bond exchange, a number of

https://doi.org/10.1021/acs.macromol.3c00482
Macromolecules 2023, 56, 4855−4873

bonds are broken and formed, transforming elastically active bonds into elastically inactive bonds (b) (green dashed bonds). The fraction of exchanged bonds is directly related to a reduction in the amount of EANS. However, there are a number of bonds that, without participating in any exchange reaction, have been totally detached from the elastically active network structure (purple bonds) or partially detached but from one bond (yellow bonds). These bonds have been deactivated and therefore have lost elastic activity. As the bond exchange progresses, the network fraction and therefore the number of network strands contributing to stress gradually decrease and the deactivated fraction increases. Eventually, a point will be reached at which no elastically active network structure remains and the stress relaxes completely. In other words, during the bond exchange process, the dynamic bonds are "cleaved" (disconnected and reconnected), leading to a decrease in "crosslinking density" (EANS), and to the formation of "dangling and soluble" (non-exchanged but elastically inactive) fractions; eventually, the network structure is disintegrated and "degelation" occurs (stress is relaxed completely).

The use of this analogy gives rise to some consequences that need to be elaborated further. First, in a crosslinking process, a certain extent of reaction conversion is needed before a network is formed (gelation); conversely, for a decrosslinking process, only a fraction of the bonds must be broken to disintegrate the network (degelation). The functionality of the monomers used to produce the material will have an influence on the process: higher functional monomers decrease the conversion at gelation; therefore, a higher extent of bond exchange will be required to relax the stress completely. The required extent of bond exchange will have an impact on the relaxation kinetics and therefore on the observed relaxation time.

Second, given that it is not necessary that all the existing bonds be exchanged for the stress to relax completely, it is not required that all the bonds in the network have exchange capabilities. In other words, a certain fraction of permanent or static bonds can be allowed in the network structure. Evidence of this was reported by Li et al.,[6] who produced materials that could relax completely when the fraction of permanent bonds remained below a certain threshold, but with slower kinetics than the material prepared without permanent bonds. However, if this fraction is excessive, a permanent network would result, and a permanent non-zero stress would remain at the end of the process even when all the bonds have been exchanged, as depicted in Figure 1d. Based on the theory of Flory for a crosslinking process, a theoretical threshold was obtained for the maximum amount of non-dynamic monomer enabling full relaxation of the stress.[6] Above this threshold, stress relaxation was incomplete, limiting the repair capabilities of the materials. With a similar reasoning, Konuray et al.[12] used the concept of permanent network to predict the residual stress and the limiting threshold of permanent bonds, with certain accuracy. This threshold will depend on the functionality of the components of the network structure.

Finally, although bonds are constantly being exchanged in the material (Figure 2), bond exchange within the deactivated fractions (i.e. "dangling" or "soluble") will produce no effect on the process of relaxing the stress from the elastically active network structure. This means that, from a kinetics point of view, the effect of bond exchange on stress relaxation will be more pronounced at the beginning of the process, when all the network strands are stretched and elastically active. This is a reformulation of the hypothesis of Parada and Zhao,[36] but in more general terms and therefore having a broader scope of application.

For all the aforementioned reasons, the same methods that are used to analyze crosslinking or network build-up processes can be used to analyze the analogous decrosslinking process taking place during stress relaxation.

Similar to the analysis of crosslinking processes,[37−39] the evolution of the network and polymer structure during a stress relaxation process can be studied using a recursive method based on the definition of structural fragments. These fragments connect to each other following certain rules and respecting certain probabilities.

The application of this concept is illustrated in Figure 3. The original distribution of fragments resulting from a step-wise

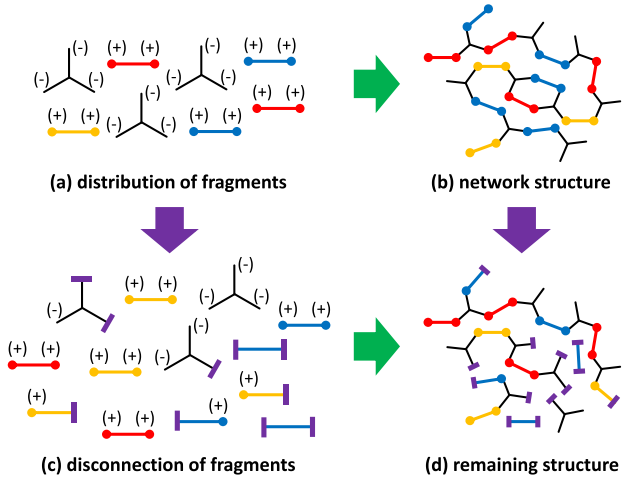

Figure 3. Schematics of the recursive method based on structural fragments, showing (a) original distribution of fragments and (b) network structure, (c) disconnection of bonds in the structural fragments, and (d) resulting network structure.

polymerization process (a) contains fragments with (+) and (−) bonds that are randomly connected to produce a probable network structure (b). Logically, the number of (+) bonds must be equal to the number of (−) bonds. It is assumed that the step-wise polymerization process is ideal, i.e., the system is stoichiometric, so that there are no pending unreacted functionalities leading to a more complex distribution of fragments, and there is no internal cyclization nor other non-ideal effects. The bond exchange process taking place during stress relaxation leads to the disconnection of bonds from one or more of the fragments (c). The resulting structure (d) may or may not have a sufficient degree of connectivity to sustain a network. Therefore, the process may lead either to a permanent network structure if a network structure remains after disconnection of all the dynamic bonds, yielding a non-zero value of stress at the end of the relaxation, or to a permanent ungelled polymer if no crosslinked network is obtained and stress is relaxed completely. This implies that there will be a fraction of fragments with (+) bonds with exchange capabilities, while another fraction can be devoid of this capability (i.e., permanent or static). As can be seen in Figure 3, some bonds can be disconnected but at different rates (blue fragments fast, yellow fragments slow). Other bonds, in contrast, may lead to permanent connections (red fragments).

https://doi.org/10.1021/acs.macromol.3c00482
Macromolecules 2023, 56, 4855−4873

The degree of connectivity of the remaining network will decrease depending on the relative contribution of dynamic versus permanent bonds, and on the extent of bond exchange. The combination of a kinetic bond exchange model with the calculated evolution of the network structure with the extent of bond exchange will reveal interesting information regarding the expected kinetic behavior of relaxation processes.

Therefore, it will be of interest to examine the effect of the feed ratio of monomers having dynamic bond exchange capabilities, r_{dyn}, and the extent of bond exchange, x, on the distribution of fragments and the resulting network architecture, if any. The process with simple relaxation kinetics will be studied first, but the effect of having bond exchange events with different kinetics will also be examined. Moreover, it will also be convenient to analyze the bond exchange process starting from a point in which a fraction of the bonds is already disconnected, as in CANs based on dissociative bond exchange reactions.

The main features of this network decrosslinking process will be highlighted in this section. A more detailed mathematical description of the model is presented in Supporting Information.

Structural Model (Simple Relaxation Process). We define a material produced from the stoichiometric reaction of h-functional dynamic D_h and j-functional static S_j monomers with f-functional monomers A_f. Reacted D_h and S_j lead to fragments with (+) bonds, while reacted A_f leads to (−) bonds. (+) bonds are randomly connected with (−) bonds. It is not required that the D_h and S_j monomers have the same functional group, but that both can react with the groups from A_f. It is required that the number of (+) bonds and (−) bonds are equal at the beginning of the process

$$h\cdot[D_h]_0 + j\cdot[S_j]_0 = f\cdot[A_f]_0 \tag{1}$$

A ratio of dynamic bonds r_{dyn} with respect to the total (+) bonds can be defined as follows

$$r_{dyn} = \frac{h\cdot[D_h]_0}{h\cdot[D_h]_0 + j\cdot[S_j]_0} \tag{2}$$

In the course of the reaction, the bond exchange process will produce a change in the concentration and distribution of the different fragments depending on the degree of connectivity. If a (+) bond from a dynamic D_h is disconnected, and then another (−) bond will be disconnected from the A_f fragments. In consequence, the concentration of (+) and (−) bonds will decrease in the course of the dynamic bond exchange process.

A distribution of D_{h-a} fragments, in which a number a of (+) bonds have been exchanged and $h-a$ bonds have not been exchanged yet, $a \in [0, h]$, can be determined from the starting D_h fragment and the extent of bond exchange/disconnection x as

$$[D_{h-a}] = [D_h]_0\cdot\binom{h}{a}\cdot(1-x)^{h-a}\cdot x^a \tag{3}$$

Likewise, a distribution of A_{f-a} fragments, in which a number a of (−) bonds have been exchanged and $f-a$ bonds have not been exchanged yet, $a \in [0, f]$, can be determined from the starting A_f fragment and the extent of bond exchange/disconnection x as

$$[A_{f-a}] = [A_f]_0\cdot\binom{f}{a}\cdot(1-r_{dyn}\cdot x)^{f-a}\cdot(r_{dyn}\cdot x)^a \tag{4}$$

Logically, the concentration of fragments with static bonds is preserved $[S_j] = [S_j]_0$.

The total number of (−) bonds of A_f fragments fulfills this condition

$$[A_f]_0\cdot f\cdot(1-r_{dyn}\cdot x) = \sum_{a=0}^{f}([A_{f-a}]\cdot(f-a)) \tag{5}$$

The concentration of (+) bonds from D_h fragments fulfills this condition

$$[D_h]_0\cdot h\cdot(1-x) = \sum_{a=0}^{h}([D_{h-a}]\cdot(h-a)) \tag{6}$$

The total number of exchanged (−) and (+) bonds is equal in the course of the bond exchange process. In consequence, the remaining amount of non-exchanged (+) and (−) bonds must also be equal

$$[A_f]_0\cdot f\cdot(r_{dyn}\cdot x) = [D_h]_0\cdot h\cdot x$$
$$[A_f]_0\cdot f\cdot(1-r_{dyn}\cdot x) = [D_h]_0\cdot h\cdot(1-x) + [S_j]_0\cdot j \tag{7}$$

From the abovementioned expressions, it can be deduced that, if there is a fraction of static bonds, $r_{dyn} < 1$, a fraction of (−) bonds from the A_f fragments will not be exchanged.

The recursive methodology supposes a "fishing" process[37] in which the probability of capturing the different fragments with (−) or (+) bonds is calculated using the following equations

$$P^{(-)}_{A_{f-a}} = \frac{(f-a)\cdot[A_{f-a}]}{[A_f]_0\cdot f\cdot(1-r_{dyn}\cdot x)}$$
$$P^{(+)}_{D_{h-a}} = \frac{(h-a)\cdot[D_{h-a}]}{[D_h]_0\cdot h\cdot(1-x) + [S_j]_0\cdot j}$$
$$P^{(+)}_{S_j} = \frac{j\cdot[S_j]}{[D_h]_0\cdot h\cdot(1-x) + [S_j]_0\cdot j} \tag{8}$$

The analysis based on the definition of expected weight makes it possible to define easily a condition for the degelation during the decrosslinking process. The expected weights pending from the (+) and (−) bonds, $W^{(+)}$ and $W^{(-)}$ respectively, are calculated from the probability of "fishing" or capturing fragments with a complementary bond and the associated mass of the fragments, including the *expected* weights issuing from the remaining bonds of the captured fragments

$$W^{(+)} = \sum_{a=0}^{f}(P^{(-)}_{A_{f-a}}\cdot(M_{A_f} + (f-a-1)\cdot W^{(-)}))$$
$$W^{(-)} = P^{(+)}_{S_j}\cdot(M_{S_j} + (j-1)\cdot W^{(+)}) + \sum_{a=0}^{h}(P^{(+)}_{D_{h-a}}\cdot(M_{D_h} + (h-a-1)\cdot W^{(+)})) \tag{9}$$

By rearranging these expressions in matrix form for variables $W^{(+)}$ and $W^{(-)}$, the following coefficient matrix M is obtained

$$M = \begin{pmatrix} 1 & m_{(+,-)} \\ m_{(-,+)} & 1 \end{pmatrix} \tag{10}$$

https://doi.org/10.1021/acs.macromol.3c00482
Macromolecules 2023, 56, 4855−4873

where the coefficients $m_{(+,-)}$ and $m_{(-,+)}$ are determined as

$$m_{(+,-)} = -\sum_{a=0}^{f} (P^{(-)}_{A_{f-a}} \cdot (f - a - 1))$$

$$m_{(-,+)} = -P^{(+)}_{S_j} \cdot (j - 1) - \sum_{a=0}^{h} (P^{(+)}_{D_{h-a}} \cdot (h - a - 1)) \quad (11)$$

The determinant of matrix M is calculated as $|M| = 1 - m_{(+,-)} \cdot m_{(-,+)}$.

At the beginning of the exchange process, $x = 0$, the system is crosslinked and $|M| < 0$. The value of $|M|$ increases in the course of the exchange process until a threshold value of conversion x^* is reached, when $|M| = 0$. At this point, degelation occurs, and it can be demonstrated that

$$x^* = 1 - \sqrt{\frac{1 - (1 - r_{dyn}) \cdot (j - 1) \cdot (f - 1)}{r_{dyn} \cdot (h - 1) \cdot (f - 1)}} \quad (12)$$

By analogy with a crosslinking process, this can be expressed as

$$x^* = 1 - x_{gel} = 1 - \sqrt{\frac{1}{(f^* - 1) \cdot (h - 1)}} \quad (13)$$

It can be seen that the expression $x_{gel} = 1 - x^*$ is equivalent to the well-known Flory–Stockmayer expression for the conversion at gelation in a crosslinking process for a stoichiometric system involving the dynamic species D_h with functionality h and a species with a functionality f^*. The latter is the equivalent functionality of a branched oligomer obtained from the reaction of a monomer A_f with the fraction of monomer with static bonds S_j (if present), calculated as

$$f^* = 1 + \frac{r_{dyn} \cdot (f - 1)}{1 - (1 - r_{dyn}) \cdot (j - 1) \cdot (f - 1)} \quad (14)$$

when $r_{dyn} = 1$, $f^* = f$ and then the equivalence with the crosslinking process is more clearly seen.

In a fashion similar to the work by Li et al.,[6] a critical threshold of dynamic bonds r_{dyn} can be defined, $r_{dyn}{}^*$, at which degelation takes place once all the bonds have been exchanged, $x^* = 1$

$$r_{dyn}{}^* = 1 - \frac{1}{(f - 1) \cdot (j - 1)} \quad (15)$$

This expression is more general than the one provided by Li et al.[6] and is also consistent with the work of Konuray et al.[12] It is not surprising that $r_{dyn}{}^* = 1 - r_c$, where r_c is the critical ratio of reactive groups from static monomer S_j with respect to reactive groups from A_f monomer leading to network formation at the end of a polymerization process in off-stoichiometric A_fS_j step-wise systems.[37]

If the fraction of dynamic bonds is $r_{dyn} > r_{dyn}{}^*$, then degelation will occur at $x^* < 1$ and full stress relaxation will be observed. If $r_{dyn} < r_{dyn}{}^*$, the fraction of static/permanent bonds will be sufficient to ensure the existence of a permanent network structure once $x = 1$, resulting in incomplete stress relaxation.

In order to calculate the network parameters in the course of a stress relaxation process, it is necessary to define the extinction probabilities of the (+) and (−) bonds, $Z^{(+)}$ and $Z^{(-)}$, respectively. Each Z is defined as the probability that the branch connected to the bond has finite continuation and is calculated from the probability of "fishing" fragments with complementary bonds and the associated extinction probabilities of the remaining bonds as

$$Z^{(+)} = \sum_{a=0}^{f} (P^{(-)}_{A_{f-a}} \cdot (Z^{(-)})^{f-a-1})$$

$$Z^{(-)} = P^{(+)}_{S_j} \cdot (Z^{(+)})^{j-1} + \sum_{a=0}^{h} (P^{(+)}_{D_{h-a}} \cdot (Z^{(+)})^{h-a-1}) \quad (16)$$

At the beginning of the stress relaxation process, $Z^{(+)}$ and $Z^{(-)}$ take a value of 0 (for an ideal crosslinked network without defects), which increases to 1 when $x = x^*$ (degelation).

The calculation of the most relevant statistical averages of the crosslinked network during the stress relaxation is the concentration of network strands, n_{strand}, and the concentration of EANS, n_{EANS}. The total number of network strands is calculated from the crosslinks present in the system, taking into consideration the fragments issuing at least three non-exchanged bonds with infinite continuation

$$n_{strand} = \sum_{a=0}^{f-3} \left([A_{f-a}] \cdot \sum_{n=3}^{f-a} \left(\phi_n \cdot \left(\frac{n}{2}\right) \cdot \binom{f-a}{n} \cdot (1 - Z^{(-)})^n \cdot (Z^{(-)})^{f-a-n} \right) \right) + [S_j] \cdot \sum_{n=3}^{j} \left(\phi_n \cdot \left(\frac{n}{2}\right) \cdot \binom{j}{n} \cdot (1 - Z^{(+)})^n \cdot (Z^{(+)})^{j-n} \right) + \sum_{a=0}^{h-3} \left([D_{h-a}] \cdot \sum_{n=3}^{h-a} \left(\phi_n \cdot \left(\frac{n}{2}\right) \cdot \binom{h-a}{n} \cdot (1 - Z^{(+)})^n \cdot (Z^{(+)})^{h-a-n} \right) \right) \quad (17)$$

The factor ϕ_n is equal to 1 for the calculation of the total network strands. This factor ϕ_n is, in fact, equivalent to the front factor commonly found in the expressions for the determination of the elastic modulus, and a value $\phi_n = 1$ would be equivalent to the affine network model. However, for the determination of n_{EANS}, the same expression will be used but with $\phi_n = 1 - 2/n$, that is, following the phantom network model. There are strong arguments in favor of the phantom network model in terms of the effective elastic contribution of the network strands, especially when crosslinks with different functionality may be found in the network structure.[40,41] The phantom network model has also been shown to provide a reasonable description of the elastic properties of vitrimers.[30,42]

It is assumed that the fraction of EANS with respect to the beginning of the process can be used as an estimate of the stress relaxation

$$f_{stress} = \frac{n_{EANS}}{n_{EANS}(x = 0)} \quad (18)$$

Other parameters of interest, although not influencing the stress response of the material, can be determined. Two such parameters are soluble fraction w_{sol}, accounting for the material

https://doi.org/10.1021/acs.macromol.3c00482
Macromolecules 2023, 56, 4855−4873

which is totally detached from the initial network structure, and the fraction of dangling chains w_{dang}, which accounts for the material connected to the network structure by only one bond. We can define the total fraction of "mobile" material, without elastic activity, $w_{mobile} = w_{sol} + w_{dang}$, and the fraction of network material with an elastic contribution $w_{net} = 1 - w_{mobile}$.

In addition to monitoring the evolution of these parameters during the stress relaxation process, it is of interest to determine their value at the end of the relaxation process ($x = 1$) when $r_{dyn} < r_{dyn}^*$. Whereas f_{stress}^* represents the remaining stress due to the presence of a non-relaxing and permanent network, w_{net}^* represents the fraction of material contributing to the remaining stress.

It must be stressed that the expressions obtained above for a simple combination of A_f (−), D_h (+) and S_j (+) fragments can be generalized for mixtures of fragments with different functionalities. In the same way as for the generalized expressions for the crosslinking processes in ideal step-wise polymerizations,[37,39] it can be shown that the expressions for x^*, f^*, and r_{dyn}^* take the same form for mixtures of fragments with average functionalities f'' for (−) fragments, h'' for dynamic (+) fragments, and j'' for static (+) fragments. The average functionality is defined as the second moment of the monomer functionality. For instance, for the (−) fragments

$$f'' = \frac{\sum_i ([A_{f_i}]\cdot f_i^2)}{\sum_i ([A_{f_i}]\cdot f_i)} \tag{19}$$

A full derivation of all the expressions shown in this section can be found in Supporting Information.

Relaxation Kinetics Model (Simple Relaxation Process). In order to derive a kinetic model, it is assumed that the rate of bond exchange does not alter the network structure of the material and that it proceeds under steady state conditions, that is

$$r_{exch} = k_{exch}\cdot[B] \simeq \text{constant} \tag{20}$$

Where $[B]$ is the total concentration of bonds that can be exchanged in the network, which remains constant, and k_{exch} is the rate constant for the exchange process, which is determined mostly by the rate-limiting step of the bond exchange reaction. It can depend on the concentration of active catalytic species and other factors affecting the process such as the intrinsic mobility of the network structure.[5,15,17]

In the present structural modeling, it is assumed that the bonds in the network at the beginning of the stress relaxation process are being gradually exchanged to yield new bonds that do not contribute to the elastic response of the material. This reduces the concentration of effective crosslinks or EANS. Therefore, we can redefine the rate law of the bond exchange reactions by considering that, in the apparent network de-crosslinking process, the non-exchanged bonds with concentration $\lceil B_{n\text{-}e}\rceil$ are transformed into exchanged bonds $\lceil B_e\rceil$, while keeping the total concentration of bonds constant

$$\lceil B_{n\text{-}e}\rceil + \lceil B_e\rceil = \lceil B\rceil = \text{constant}$$
$$\frac{d\lceil B_{n\text{-}e}\rceil}{dt} + \frac{d\lceil B_e\rceil}{dt} = \frac{d\lceil B\rceil}{dt} = 0 \tag{21}$$

We can therefore write a rate expression for the non-exchanged bonds, $\lceil B_e\rceil$, such as

$$-\frac{d\lceil B_{n\text{-}e}\rceil}{dt} = k_{exch}\cdot\lceil B_{n\text{-}e}\rceil \tag{22}$$

If we define $\lceil B_{n\text{-}e}\rceil = \lceil B\rceil\cdot(1 - x)$, where x is the extent of the exchange process from the beginning of the stress relaxation, this expression can be rewritten as

$$\frac{dx}{dt} = k_{exch}\cdot(1 - x) \tag{23}$$

However, the bond exchange process leads to the increasing concentration of not only exchanged bonds but also "deactivated" bonds that are not contributing to the elastic response of the material, i.e., they do not belong to the network structure with EANS (see Figure 2). Bond exchange events taking place within these elastically inactive fractions of material will not produce a change in the structure of the material. It follows that only the bond exchange events taking place within the network structure will produce an effective change in the state of elastic response of the material. In consequence, the effectiveness of the bond exchange will be higher at the beginning of the process, where all the material contributes to the elastic response, than at the end of the process, where only a reduced fraction of the material contributes to the elastic response. The rate expression is therefore modified as

$$\frac{dx}{dt} = f_{eff}\cdot k_{exch}\cdot(1 - x) \tag{24}$$

where the factor f_{eff} represents the likelihood that a bond exchange takes place within the network structure so that an appreciable change occurs in the elastic response of the material. f_{eff} takes a value of 1 at the beginning of the relaxation process, when all the network strands are elastically active, and 0 at the end, when all the strands have been deactivated. A detailed definition of f_{eff} is provided in the Supporting Information.

Integration of the rate expression for a discrete time-conversion range, small enough so that f_{eff} can be assumed to be constant, yields

$$\int_x^{x+\Delta x}\frac{dx}{(1 - x)} = \int_t^{t+\Delta t} f_{eff}\cdot k_{exch}\cdot dt$$
$$\Delta t = \frac{-\ln\left(1 - \frac{\Delta x}{1 - x}\right)}{f_{eff}\cdot k_{exch}}$$
$$\Delta x = (1 - x)\cdot(1 - \exp(-f_{eff}\cdot k_{exch}\cdot\Delta t)) \tag{25}$$

The two abovementioned expressions can be utilized to determine numerically $x_{i+1} = x_i + \Delta x$ for a given $t_{i+1} = t_i + \Delta t$ or vice versa. f_{eff} can be evaluated from the structural analysis at x_i. Initial conditions are $t_0 = 0$ and $x_0 = 0$, unless stated otherwise.

The calculated stress relaxation curves will be fitted to stretched exponential functions[6,16,42] with the shape

$$f_{stress} = f_{stress}^* + (1 - f_{stress}^*)\cdot\exp\left(-\left(\frac{t}{\tau}\right)^{\beta}\right) \tag{26}$$

where f_{stress}^* is the residual stress, τ is the characteristic relaxation time, and β is the shape factor, typically representing a distribution of relaxation times in a structure relaxation process.[37] f_{stress}^* is calculated from the structural model, τ is determined as the time at which it is verified that

https://doi.org/10.1021/acs.macromol.3c00482
Macromolecules 2023, 56, 4855−4873

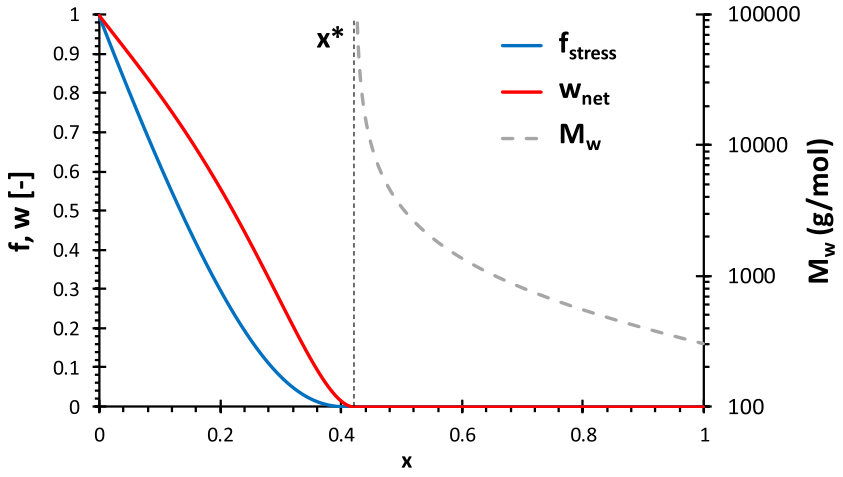

Figure 4. Calculation of structural parameters during a bond exchange process for an A_4D_2 system, with respect to the extent of the bond exchange process.

$f_{stress} = f_{stress}^{*} + (1 - f_{stress}^{*})\cdot\exp(-1)$ (from the condition $t = \tau$; notice that in the absence of permanent network, $f_{stress}^{*} = 0$, the condition is $f_{stress} \simeq 0.37$), and β is determined by numerical fitting of the function to the calculated relaxation curve between $t = 0$ and $t = \tau$.

Complex Relaxation Processes. Let us consider an A_f fragment (−) that is combined with two dynamic monomers $D1_h$ and $D2_i$ (+) with different dynamic functionalities and bond exchange kinetics and a static monomer S_j (+). The following balance holds

$$h\cdot[D1_h]_0 + i\cdot[D2_i]_0 + j\cdot[S_j]_0 = f\cdot[A_f]_0 \tag{27}$$

A ratio of dynamic bonds r_{dyn} with respect to the total (+) bonds can be defined as follows

$$r_{dyn} = \frac{h\cdot[D1_h]_0 + i\cdot[D2_i]_0}{h\cdot[D1_{1,h}]_0 + i\cdot[D2_i]_0 + j\cdot[S_j]_0} \tag{28}$$

The change in the distribution and concentration of the different fragments is calculated as

$$[D1_{h-a}] = [D1_h]_0\cdot\binom{h}{a}\cdot(1 - x_1)^{h-a}\cdot {x_1}^{a}$$

$$[D2_{i-a}] = [D2_i]_0\cdot\binom{i}{a}\cdot(1 - x_2)^{i-a}\cdot {x_2}^{a}$$

$$[A_{f-a}] = [A_f]_0\cdot\binom{f}{a}\cdot(1 - r_{dyn}\cdot x)^{f-a}\cdot(r_{dyn}\cdot x)^{a} \tag{29}$$

where

$$x = r_1\cdot x_1 + r_2\cdot x_2$$

$$r_1 = \frac{h\cdot[D1_h]_0}{h\cdot[D1_h]_0 + i\cdot[D2_i]_0} \qquad r_2 = 1 - r_1 \tag{30}$$

The capture probabilities of the (−) and (+) fragments are defined in a similar way as in eq 8. In particular, the definition of $P_{A_{f-a}}^{(-)}$ is unchanged. The capture probabilities of the (+) fragments, $P_{D1_{h-a}}^{(+)}$, $P_{D2_{i-a}}^{(+)}$, and $P_{S_j}^{(+)}$, need to be reformulated by considering the contribution of $D1_{h-a}$, $D2_{i-a}$ and S_j fragments with (+) bonds. The expressions for the calculation of the extinction probabilities $Z^{(+)}$ and $Z^{(-)}$ as well as the rest of the structural parameters also need to be modified accordingly. These extra definitions are provided in the Supporting Information.

Given that there are now two relaxation events, the kinetic model is modified as follows

$$\Delta x_1 = (1 - x_1)\cdot(1 - \exp(-f_{eff,1}\cdot k_{exch,1}\cdot\Delta t))$$

$$\Delta x_2 = (1 - x_2)\cdot(1 - \exp(-f_{eff,2}\cdot k_{exch,2}\cdot\Delta t))$$

$$\Delta x = r_1\cdot\Delta x_1 + r_2\cdot\Delta x_2 \tag{31}$$

The rate constants $k_{exch,1}$ and $k_{exch,2}$ will be different for each of the dynamic fragments. The effectiveness factors are defined in the Supporting Information.

Relaxation of Dissociative CANs. In dissociative equilibrium reactions, the concentration of available dynamic bonds depends on the contribution of the forward reaction (bond formation) and backward reaction (dissociation). An equilibrium between the two reactions may eventually be established at a given temperature. A real decrosslinking takes place when the temperature is increased, eventually leading to degelation.[31,34]

Based on previous analyses,[33,34] the following reaction scheme $A + B \rightleftarrows C$ can be used to define the concentration of dissociated species $[A] = [A]_0\cdot x$ or $[B] = [B]_0\cdot x = [A]_0\cdot x$ and the associated species $[C] = [A]_0\cdot(1 - x)$, where x is the extent of dissociation (for consistency with the structural model).

$$\frac{d[C]}{dt} = -k_{back}\cdot[C] + k_{for}\cdot[A]\cdot[B] \Rightarrow \frac{dx}{dt} = k'_{back}\cdot(1 - x) - k'_{for}\cdot x^2 \tag{32}$$

where $k_{back}' = k_{back}$ and $k_{for}' = [A]_0\cdot k_{for}$ are the rate constants (normalized with respect to the total concentration of active species in the case of k_{for}).

An equilibrium may be established, $dx/dt = 0$, with an expression as follows

$$k_{eq} = \frac{k'_{back}}{k'_{for}} = \frac{k_{back}}{k_{for}\cdot[A]_0} = \frac{{x_{eq}}^2}{1 - x_{eq}} \tag{33}$$

Given the temperature dependence of the equilibrium constant k_{eq}, it is quite usual that the initial modulus and stress in stress relaxation processes decrease with temper-

https://doi.org/10.1021/acs.macromol.3c00482
Macromolecules 2023, 56, 4855−4873

ature.[8,27] In consequence, determination of the equilibrium extent of dissociation, x_{eq}, is necessary in order to characterize the initial network structure at a given temperature. The stress relaxation process is therefore analyzed starting from this equilibrium condition $x_0 = x_{eq}$. The same expressions used for the determination of the figurative decrosslinking effect taking place during a stress relaxation process at constant temperature, as described above, can be employed in the analysis of dissociative CANs. It can be assumed that the relaxation process is described using the same kinetic equation and that it is governed by the rate of the dissociation reaction[36] with constant $k_{exch} = k_{back}$. The f_{eff} factor is defined in the same way, taking the network structure with no dissociation, $x = 0$, as reference. The kinetics of the stress relaxation process is analyzed using the same expressions, but taking $x_0 = x_{eq}$ when $t_0 = 0$.

RESULTS AND DISCUSSION

Simple Relaxation Process. The stress relaxation process of a network structure based on the reaction of an A_4 monomer with a dynamic D_2 monomer has been studied in the first place. For this system, all the (+) and (−) bonds will undergo bond exchange. The results from this analysis are illustrated in Figure 4.

It can be seen how the process starts from an unrelaxed state, in which the remaining stress f_{stress} (see eq 18) is equal to 1; no material has participated or been affected by the bond exchange yet, and therefore the fraction of network material with an elastic contribution, w_{net}, is equal to 1. As the process advances, a decrease in f_{stress} and w_{net} is observed. The process continues until $f_{stress} = 0$ and $w_{net} = 0$ at a given extent of conversion x^*. If one considered a true decrosslinking process (e.g., by heating a dissociative CAN), one would expect that, after degelation, the material would start to flow with increasing facility due to the decrease in the molecular weight (dashed line in the graph). From the stress relaxation point of view, however, the process would be over at x^*. Further bond exchange would not produce any other apparent effect. Even in creep experiments, in which the material is being permanently deformed, the structural integrity of the material would be unaffected. In consequence, from now on, the relaxation process will be analyzed only until $x = x^*$, or else until $x = 1$ if relaxation is incomplete.

As discussed in the theoretical section, it is not surprising that $x^* \simeq 0.42 = 1 - x_{gel}$, where $x_{gel} \simeq 0.58$ would be the conversion at gelation during polymerization of an $A_4{-}D_2$ reactive system. Making use of eqs 12 and 13, it can be expected that increasing the functionalities f and h of the A_f and D_h components will produce an increase in x^*. For the same reason that gelation takes place earlier in a crosslinking process, it requires a greater extent of bond exchange to relax the network structure as functionalities increase. This will be discussed later on in this work.

The presence of static or permanent bonds in the network can be analyzed using this model. Figure 5 shows the effect of the dynamic monomer content, r_{dyn}, on the relaxation of $A_4D_2S_2$ networks. A number of effects can be observed in Figure 5a: (1) starting from the network fully based on dynamic bonds, $r_{dyn} = 1$, the relaxation process reaches completion at higher extents of bond exchange and broadens with decreasing r_{dyn}, and (2) below a certain critical ratio r_{dyn}^*, relaxation is incomplete, leading to an increasing value of

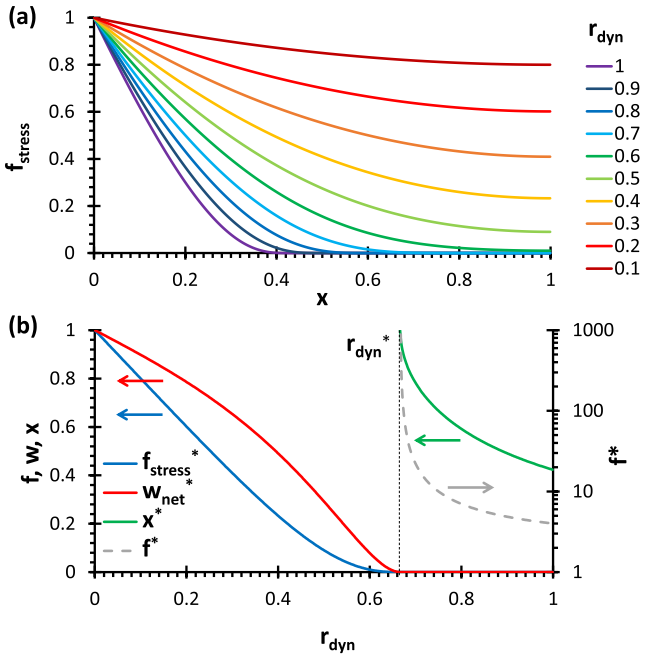

Figure 5. Effect of the ratio of dynamic monomer content, r_{dyn}, on the stress relaxation of $A_4D_2S_2$ networks (a) with respect to the extent of the bond exchange process and (b) on the different structural parameters associated with the relaxation. An equivalent weight of 100 g/equiv has been assumed for all cases.

residual stress with decreasing r_{dyn} produced by the existence of a permanent network structure. For $r_{dyn} = 0$, no stress relaxation occurs (constant $f_{stress} = 1$, not shown in the graph). The critical ratio r_{dyn}^*, obtained with eq 15, has a value of 0.667 for this $A_4D_2S_2$ system. A lower value $r_{dyn}^* = 0.5$ was reported by Li et al. in their analysis of the presence of permanent bonds in thiol-epoxy vitrimer,[6] which can be assimilated to a $A_3D_2S_2$ system; Konuray et al. reported, in contrast, a value of 0.75 for their $A_3D_2S_3$ system.[12] Both values can be exactly predicted by the general expression (15) derived in this work.

The structural effect of the ratio of dynamic bonds, r_{dyn}, depending on the presence of a static or permanent monomer, is also summarized in Figure 5b. Key structural parameters f_{stress}^*, w_{net}^*, x^*, and f^* have been plotted as a function of r_{dyn}. For $r_{dyn} > r_{dyn}^*$, the ratio of dynamic bonds is sufficiently high to ensure complete stress relaxation in any case. It can be observed that the critical conversion x^* reaches a value of 1 at $r_{dyn} = r_{dyn}^*$, and then it decreases down to the value of $x^* = 0.42$ for $r_{dyn} = 1$, the pure A_4D_2 network. When r_{dyn} approaches r_{dyn}^*, a higher extent of bond exchange is required to reach x^* and completely relax the material; this is deemed to have a significant impact on the relaxation kinetics. In parallel to the evolution of x^*, the parameter f^* (see eq 14), which is the functionality of the combined $A_4{-}S_2$ fragments at a given r_{dyn}, represents the structure of the underlying permanent ungelled polymer. f^* tends to infinity at $r_{dyn} = r_{dyn}^*$, and it decreases to $f^* = f = 4$ at $r_{dyn} = 1$. The parameter f^* might be correlated with the creep resistance of the materials.[6] Given that there is no permanent network, full recycling and reprocessing capabilities are expected within this region, enabling a more

https://doi.org/10.1021/acs.macromol.3c00482
Macromolecules 2023, 56, 4855−4873

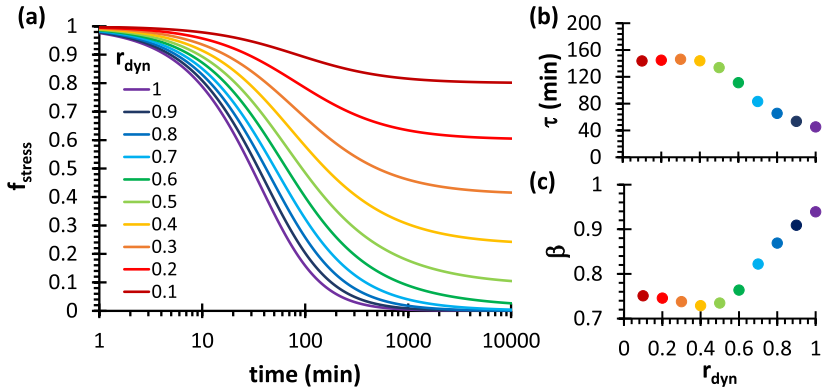

Figure 6. (a) Stress relaxation of $A_4D_2S_2$ networks for various ratios of dynamic monomer r_{dyn}, with respect to time, corresponding to the same scenario in Figure 5. A value of k_{exch} = 0.006 min^{-1} has been used for the calculation of all curves. The two side graphs (b) and (c) show the results from the fitting of the stress relaxation curves to the stretched exponential function given by eq 26.

flexible design of vitrimer materials containing only a fraction of dynamic bonds.

For $r_{dyn} < r_{dyn}^*$, stress relaxation is incomplete because of the presence of a permanent network structure. Structural parameters f_{stress}^* and w_{net}^* are determined assuming the bond exchange process is complete, x = 1. It can be observed that there is an almost linear trend of f_{stress}^* with respect to r_{dyn}, decreasing from a value of 1 at r_{dyn} = 0 to a value of 0 when $r_{dyn} = r_{dyn}^*$. However, it is observed that, in fact, f_{stress}^* reaches a value almost equal to 0 before r_{dyn}^* is reached. Therefore, quantitative or almost full stress relaxation can be achieved with an even lower r_{dyn} than predicted using eq 15, as observed by Konuray et al.[12] An extremely weak permanent network structure may exist within this range below r_{dyn}^*, but preventing unrestricted macroscopic flow all the same. It is also apparent that, while complete stress relaxation might be observed below r_{dyn}^*, the fraction of network material w_{net}^* would still be higher than 0. This raises a question as to whether recycling of vitrimer-like materials is possible below r_{dyn}^*: is it sufficient that the stress relaxes completely or else is it necessary that all the material participates in the process ($w_{net}^* = 0$), that is, $x^* \leq 1$ for $r_{dyn} \geq r_{dyn}^*$? Quantitative and efficient reshaping can be achieved in the vicinity of r_{dyn}^* in any case, given the low value of f_{stress}^*. In terms of recycling, the results from Konuray et al. suggest some recycling capabilities are possible below r_{dyn}^*,[12] but more evidence is required.

The relaxation kinetics of this system were analyzed using the simple first-order kinetics model with the correction factor f_{eff} (see eq 24). This model assumes that the extent of bond exchange conversion x and the relative rate of bond exchange dx/dt are independent from the actual concentration of dynamic bonds. The effect of the concentration of catalyst or active species, or other kinetic effects such as the effect of the network architecture on the mobility and reactivity of the species[5,15,17] is included in the value of the bond exchange rate constant, k_{exch}. In the case of the $A_4D_2S_2$ system presented in Figure 5, all the relaxation processes were simulated using a single rate constant k_{exch} = 0.006 min^{-1}. This assumes that (1) a similar concentration of active species or catalyst is present, and (2) that the replacement of a dynamic monomer with a static monomer does not lead to a change in the network structure or mobility, that is, it has no kinetic effect per se. In the absence of other side chemical effects, the kinetics of the relaxation process should be governed by structural effects as shown in Figure 5.

The kinetic model outputs given in Figure 6a show the typical sigmoidal curves of stress relaxation processes, using a logarithmic time scale. As anticipated from the previous discussion, decreasing r_{dyn} and thereby increasing x^* results in slower relaxation processes. For $r_{dyn} < r_{dyn}^*$, stress relaxation is incomplete, with increasing residual stress and with decreasing r_{dyn} (in the limiting case r_{dyn} = 0, no stress relaxation is observed, with constant f_{stress} = 1). The characteristic relaxation times τ and the residual stress f_{stress}^* were determined from the calculated curves. The curves were fitted to the stretched exponential function given by eq 26 in order to determine the shape parameter β. The values of τ and β with respect to the value of r_{dyn} have also been presented in the figure. It is also observed that τ increases with decreasing r_{dyn} up to a certain asymptotic value reached at a r_{dyn} significantly lower than r_{dyn}^*. Conversely, the value of β shows a decreasing trend with decreasing r_{dyn} and reaches an asymptotic value as well.

Interestingly, Li et al. had also reported increasing values of τ and decreasing values of β with increasing permanent monomer content[6] (that is, decreasing dynamic monomer content r_{dyn}). We simulated the relaxation of an $A_3D_2S_2$ system with values of r_{dyn} equivalent to the fraction of permanent monomers used in the work of Li et al.[6] For this system, the value of r_{dyn}^* is equal to 0.5. The results of the simulation (Figure S1 in Supporting Information) show trends consistent with the reported results. Residual stress calculated for a fraction of permanent bonds of 60 and 80% (r_{dyn} equal to 0.4 and 0.2, respectively) is 0.037 and 0.422, respectively; these values compare well with the reported data, considering the experimental uncertainty and the limited relaxation time used in the analysis.[6] The simulated curves were fitted to stretched exponential functions yielding values of β systematically higher than experimental ones, but following the same trend; the evolution of overall relaxation times was also comparable. The current model predicts exactly the same value of residual stress for an $A_3D_2S_3$ as the simplified model published by Konuray et al.,[12] showing good agreement with experimental data. A similar broadening effect was also observed, although the

https://doi.org/10.1021/acs.macromol.3c00482
Macromolecules 2023, 56, 4855−4873

existence of an additional relaxation event[12] suggests that a better modeling of the system would require the consideration of a complex relaxation process, as will be discussed in the following section. Preliminary analysis of ternary thiol-isocyanate-epoxy networks with transcarbamoylation exchange of thio-urethane bonds (results not published yet) confirms the prediction capabilities of the model. Therefore, the kinetic predictions of the model seem to be correct at least from a qualitative point of view.

The analysis of the relaxation kinetics makes it is also possible to discuss the recycling capabilities of the materials with r_{dyn} above or below r_{dyn}^*. Recycling conditions employed in the work by Li et al. enable almost quantitative stress relaxation for materials with 40% permanent bonds ($r_{dyn} = 0.6 > r_{dyn}^* = 0.5$). However, the recycling time used may fall short for 60% of permanent bonds ($r_{dyn} = 0.4 < r_{dyn}^*$), leading to significant remaining stress.[6] Nevertheless, given that the theoretical f_{stress}^* is equal to 0.037 for $r_{dyn} = 0.4$, a more satisfactory recycling might be achieved after a longer treatment. The question remains whether it is necessary for the samples to have the ability to relax completely, that is, there shall be no barrier to macroscopic molecular flow ($r_{dyn} > r_{dyn}^*$), or else recycling is possible as long as stress can be relaxed almost quantitatively ($r_{dyn} \leq r_{dyn}^*$ but in close vicinity to r_{dyn}^*, see Figure 5). Preliminary results by Konuray et al. suggest that this might be possible.[12] Even if the material is fully recyclable, insufficient processing time/temperature might lead to inefficient mending/recycling.[30] The existence of an underlying network structure, as noted by Strachota,[32] may not be a drawback for applications such as self-healing as long as a sufficient fraction of the material (having sufficient mobility) can participate in the process. This is a subject that deserves further investigation.

Although it is not the purpose of this work to analyze the kinetics of creep experiments, it can be hypothesized that the control of undesired creep reported in the literature by means of the incorporation of permanent bonds in the network structure can also be rationalized by the same kinetic effect observed in stress relaxation. As seen in Figure 5, reducing r_{dyn} leads to higher x^*, which makes it longer to reach a state of apparent flowing ability. The parameter f^*, defined previously, can also be interpreted as the average number of bonds of the fragments that can be fully detached from the network structure. As such, it can be relevant also for creep dynamics, as it would play a role similar to the molecular weight or viscosity. The higher the value of f^*, the more bonds would need to be disconnected/exchanged to produce fragments that can flow. If creep is to be completely avoided, it is necessary that $r_{dyn} < r_{dyn}^*$.

Figure 7 compares the combined effect of the network structure and the dynamic monomer content r_{dyn}. Figure 7a shows the critical conversion at stress relaxation, x^*, which can only be defined for $r_{dyn} > r_{dyn}^*$, calculated using eq 12 or eqs 13 and 14. It can be clearly observed that the value of r_{dyn}^*, determined as the point when $x^* = 1$, becomes lower when the overall network structure becomes looser, but does not depend on the functionality h of the dynamic fragment D_h. This can be of economical relevance especially when the dynamic monomer is costly, because materials with full relaxation

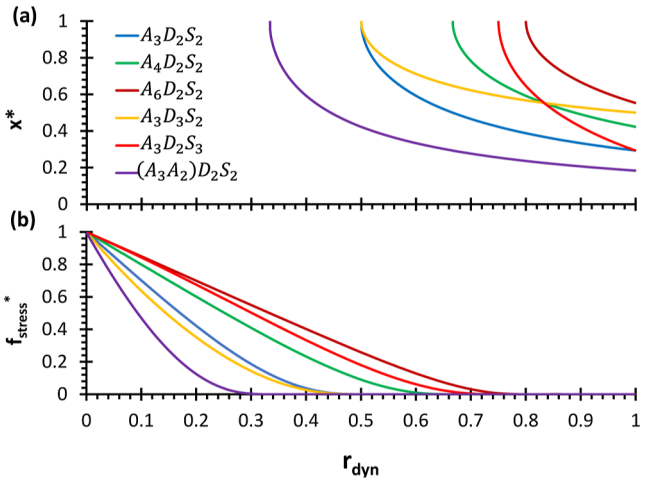

Figure 7. Determination of (a) x^* and (b) f_{stress}^* for different $A_f D_h S_j$ networks, depending on the dynamic monomer content, r_{dyn}.

capabilities can be defined with even lower contribution from the dynamic component. Figure 7a also shows that x^* is also lower for networks with low crosslinking density. This should have a direct effect on the relaxation kinetics of the different networks. Additional kinetic effects can be expected due to the enhanced chain mobility.[17] However, excessive loosening of the network structure will limit the overall thermal–mechanical properties of the materials. In Figure 7b, it can be observed that all the networks exhibit a similar trend of f_{stress}^* for $r_{dyn} < r_{dyn}^*$, with values approaching 0 as r_{dyn} approaches r_{dyn}^*. This makes it possible to easily estimate the residual f_{stress}^* at a given r_{dyn} relative to r_{dyn}^*.

Stress relaxation curves have been calculated for $A_f D_2$ systems by (1) changing the functionality of A_f monomers (Figure S2 in Supporting Information and Figure 8a) and (2) for different ratios of A_2 and A_4 monomers (Figure S3 in Supporting Information and Figure 8b). Decreasing the average functionality of A_f results in a decrease in x^* and, assuming equal k_{exch}, lower relaxation times (Figure 8a). The same can be stated for A_2–A_4 mixtures (Figure 8b). However, the kinetic effect in real systems can be substantially higher,[15,17] due to the enhancement of the rate of bond exchange promoted by the higher mobility of the network structure. In fact, both the functionality of the components and the overall crosslinking density can have an influence on the relaxation kinetics.[17] With respect to the shape of the curves, values of β between 0.85 and 0.95 are obtained, in line with other reported values.[16,43] Interestingly, the value of β decreases systematically with increasing content of A_2 in A_2–A_4 mixtures.

In vitrimers based on transesterification reactions, it has been suggested that the network should be allowed to reach equilibrium before their properties are analyzed. This is because the structure and properties can change due the existence of additional exchange sites in one or more of the components, which would lead to a rearrangement of the network structure into another one with a different distribution of structural fragments and therefore different crosslinking density and soluble fraction.[29,30] In order to simulate this effect, we have analyzed a network with a mixture of A_2–A_3 components (average functionality 2.5) with a dynamic

https://doi.org/10.1021/acs.macromol.3c00482
Macromolecules 2023, 56, 4855–4873

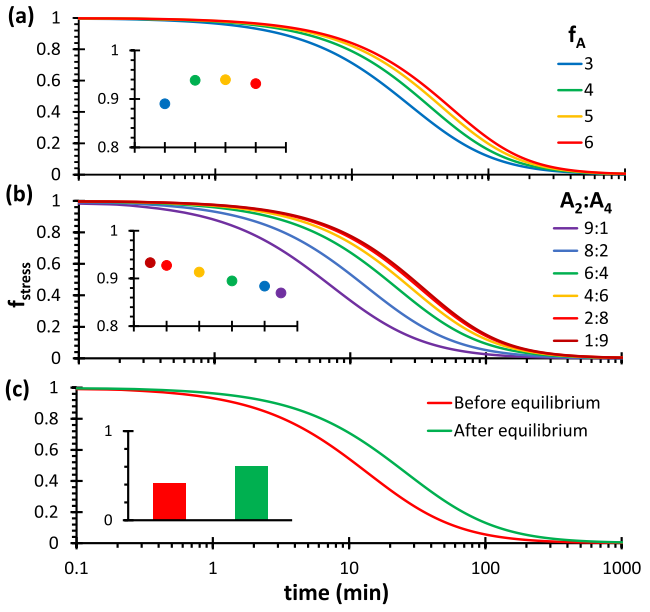

Figure 8. Stress relaxation of A_fD_2 networks with (a) different functionality f of the A_f, (b) different molar ratio of A_2 and A_4 components and (c) $(A_2A_3)D_2$ network before and after equilibrium, with a dynamic monomer with up to 4 possible exchange sites. An equivalent weight of 100 g/equiv has been assumed for all cases. A value of k_{exch} = 0.006 min^{-1} has been used for the calculation of all curves. The insets in (a) and (b) show the value of β for the different compositions. The inset in (c) shows the calculated value of n_{strand} before and after equilibrium.

component D_2 with two additional exchange sites (Figure 8c). A distribution of D_h fragments has been created assuming random occupation of all the exchange sites (a binomial distribution with h ranging from 0 to 4 and a fraction of occupied sites of 0.5). When the original network and the one with redistributed bonds are compared, a certain increase is observed in crosslinking density (see inset in Figure 8c) and the formation of a soluble fraction, as expected.[29,30] Such an increase in crosslinking is expected to produce a decrease in the rate of stress relaxation due to an increase in the required extent of bond exchange, as is indeed observed. The effect of the network rearrangement has already been observed in 3D-printable vitrimers based on transesterification.[44,45] However, the effect on kinetics may be more relevant than the one shown in the figure due to the additional kinetic effect of reduced network mobility.

Having reached this point, the validity of the kinetic model (see eq 24) should be discussed in more detail. It has been verified (Figure S4 in Supporting Information) that a sigmoidal shape is produced whether the correction factor f_{eff} is used or not. In addition, similar trends are obtained in τ and β with respect to r_{dyn}. Therefore, it can be argued that these observed kinetic effects depending on r_{dyn} have a structural origin and are not determined by the kinetic model. The effects of monomer functionality also evidence intrinsic structural trends that are generally observed.[15,17]

Model predictions yield values of β around 0.9−1 for simple systems (i.e., single dynamic component D_h) with r_{dyn} = 1. This compares well with the commonly assumed value of β = 1, equivalent to a single Maxwell relaxation element, for systems that have a simple relaxation behavior.[36,46] Predictions also compare well with the fitting of relaxation data from the literature to the stretched exponential function yields values of β around 0.8−0.95.[13,16,43] In the absence of f_{eff}, the predicted shape of the relaxation curves is too sharp and are not realistic at all, yielding values of β > 1 (Figure S4 in Supporting Information). In consequence, the use of such a correction factor, based on the stress-dependent effectiveness of the dynamic bond exchange, provides a reasonable approximation to the stress relaxation phenomenon. It is also observed that the effect of f_{eff} becomes evident only when 30−40% of the stress has been relaxed. Alternate definitions of f_{eff} produce similar effects but yield somewhat different values of β (see Figure S4 in Supporting Information). Therefore, it could be possible to match bond exchange kinetics with stress relaxation kinetics in the initial stages of the relaxation process regardless of the exact definition of f_{eff}. The use of other network structure analysis methods could help to clarify the exact role of the kinetics of bond exchange reactions on the stress relaxation.

Values of β < 1 are also systematically obtained for mixtures of dynamic components with r_{dyn} = 1 and also for r_{dyn} < 1. This leads to an apparent distribution of relaxation times,[14] as it is commonly assumed in the analysis of mechanical or dielectric relaxation processes.[37] However, such distribution results from the complex interplay between network structure, dynamic bond content, and simple bond exchange dynamics, not from a

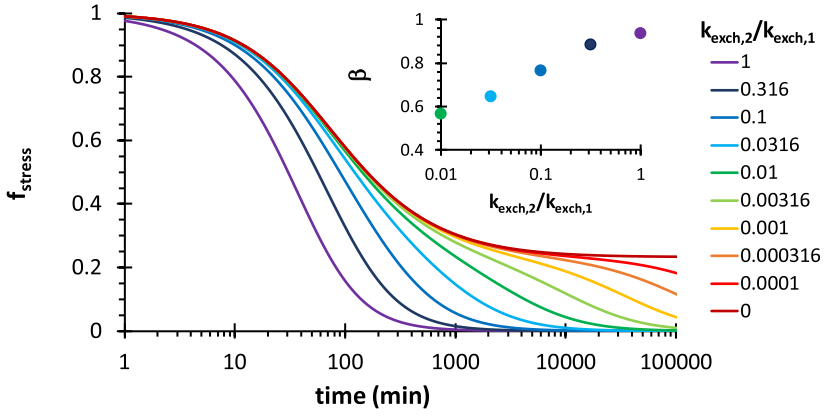

Figure 9. Stress relaxation of $A_4D1_2D2_2$ networks with a fixed ratio r_{dyn1} of 0.4 and different ratios of exchange constants $k_{exch,2}/k_{exch,1}$, and setting $k_{exch,1}$ = 0.006 min^{-1} has been used for the calculation of all curves. An equivalent weight of 100 g/equiv has been assumed for all cases. The insets show the value of β different materials.

https://doi.org/10.1021/acs.macromol.3c00482
Macromolecules 2023, 56, 4855−4873

complex relaxation kinetics behavior. In contrast, lower values of β are obtained for apparently simple relaxation processes.[6,15] This may be indicative of a certain structural and kinetic complexity of the stress relaxation process (i.e., having a distribution of relaxation kinetic events). These issues will be discussed in the following section.

Complex Relaxation Processes. In this section, we will first examine the main features of complex relaxation scenarios using D_h components with different rates of relaxation. The results of the modelling will then be discussed by comparison with complex relaxation systems already reported in the literature.[8,12−15,47]

The analysis focuses on the study of $A_4D1_2D2_2$ systems with different ratios of $D1_2$ component, r_1, and with different ratios of bond exchange rate constant of component $D2_2$ with respect to that of $D1_2$, $k_{exch,2}/k_{exch,1}$. First of all, we have studied the effect of the difference of bond exchange kinetics of the two dynamic components on the relaxation of materials for a fixed r_1 of 0.4, and no permanent bonds present $r_{dyn} = 1$. As can be seen in Figure 9, when the rate of the two exchange processes is equal, the produced curve is identical to the one shown in Figure 6 with $r_{dyn} = 1$, that is, a relaxation process with a single dynamic monomer. When $k_{exch,2}/k_{exch,1}$ decreases, the relaxation process becomes slower and the curve broadens (see the decreasing value of β in the inset), maintaining a unimodal relaxation profile. As $k_{exch,2}/k_{exch,1}$ approaches 0.01, the relaxation gradually evolves into a two-step process, its bimodality increasing with decreasing $k_{exch,2}/k_{exch,1}$. In the limit, when $k_{exch,2}/k_{exch,1} = 0$, a non-zero asymptotic value of f_{stress} is reached, which makes the process identical to the one with a single dynamic component and a static (permanent) component with $r_{dyn} = 0.4$ (see Figure 6). Therefore, it appears that the simple relaxation processes discussed in the previous section are but a particular case of a more general scenario in which the apparently static bonds (i.e., bonds contained in $D2_2$) can also be exchanged at a much lower rate. It can also be observed (see Figure S5 in Supporting Information) that, when $k_{exch,2}/k_{exch,1}$ decreases, a higher bond conversion is required overall in order to relax the material. In consequence, almost complete bond exchange of $D1_2$ may be required, with only marginal contribution of $D2_2$ if the difference in rate of bond exchange is considerable.

Interestingly, similar results were reported in the analysis of CANs based on disulfide bond exchange with permanent bonds, in which an additional relaxation step was related to the additional bond exchange by transesterification.[12] The results in Figure 9 also evidence that such complex relaxation processes can span several decades in time. In consequence, complete characterization of such effects may require the analysis at different temperatures.[12] Other researchers did not observe such apparently complex behavior but, they reported intermediate relaxation kinetics if the difference in bond exchange rate between the different components was not excessive.[13−15,47] Van Lijsebetten et al. rationalized their somewhat complex relaxation behavior by the existence of processes with distinct relaxation kinetics, which was modeled by fitting the data to multiple Maxwell elements.[8]

Such complex behavior may stem not only from the existence of clearly distinct bond exchange kinetics but also from the composition of the network structure. To make this point clearer, the effect of the ratio of the first dynamic component, r_1, was simulated for of $A_4D1_2D2_2$ networks, with different ratios of $k_{exch,2}/k_{exch,1}$. The results in Figure 10a

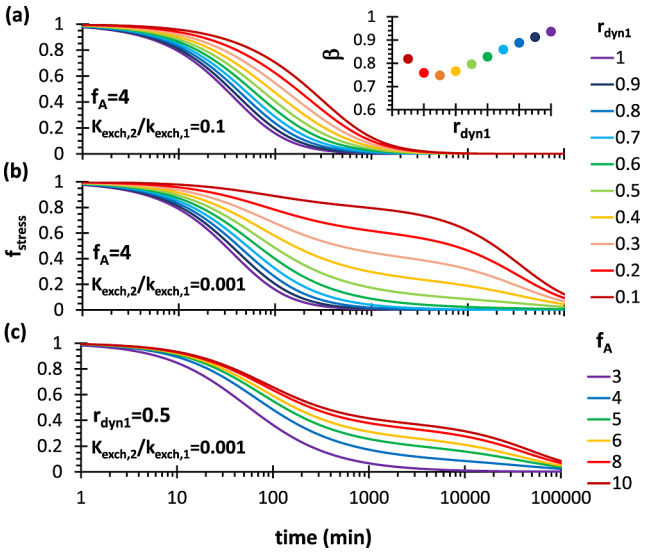

Figure 10. Stress relaxation of $A_4D1_2D2_2$ networks with variable ratios of $D1_2$ component, r_{dyn1}, a fixed ratio $k_{exch,2}/k_{exch,1}$ equal to (a) 0.1 and (b) 0.001 respectively. The inset in (a) shows the effect of r_{dyn1} on the shape parameter β for $k_{exch,2}/k_{exch,1} = 0.1$. The lower graph (c) shows the stress relaxation of $A_4D1_2D2_2$ networks with $r_{dyn1} = 0.5$, $k_{exch,2}/k_{exch,1} = 0.001$, and varying functionality of A_f component. $k_{exch,1} = 0.006$ min^{-1} has been used for the calculation of all curves. An equivalent weight of 100 g/equiv has been assumed for all cases.

evidence that, when $k_{exch,2}/k_{exch,1} = 0.1$, the relaxation process is apparently simple, with a clear broadening of the curves in the intermediate compositions (see the evolution of β in the inset in Figure 10a). In contrast, when $k_{exch,2}/k_{exch,1} = 0.001$ (Figure 10b), a stronger broadening effect is observed and a complex two-step relaxation becomes clearly apparent for r_1 lower than 0.6−0.5. Figure 10c shows the effect of the functionality f of the A_f component for $r_{dyn1} = 0.5$ and $k_{exch,2}/k_{exch,1} = 0.001$. The complexity of the relaxation process is evidenced for increasing values of f. This shows clearly that different results can be expected when crosslinking simple molecules, rather than larger molecules or even polymer chains.

The results from the analysis based on simple relaxation processes can serve as preliminary design criteria for complex processes. It is possible to calculate r_{dyn}^* using eq 15 and considering the functionality of the common component A_f and that of the second, slow-relaxing component $D2_h$, which would be acting like the static (permanent) component. As a matter of fact, one should not expect a complex bimodal behavior for $r_1 > r_{dyn}^*$, since the participation of the second component would not be required for the relaxation of the process; the bond exchange process of the first component alone guarantees that the stress would relax completely (see Figures 10 and also 5 and 6), regardless of whether the second component participates or not. On the contrary, for $r_1 < r_{dyn}^*$, the bond exchange process of the first component alone is not sufficient to relax the stress completely. A complex two-step behavior would only be observed if there is a large difference in kinetics, that is, $k_{exch,2}/k_{exch,1}$ is sufficiently low; if the difference is not too large, then an apparently unimodal relaxation behavior would be observed. The relevant effect of the functionality of the components on the apparent kinetics behavior makes it necessary to take this factor into

https://doi.org/10.1021/acs.macromol.3c00482
Macromolecules 2023, 56, 4855−4873

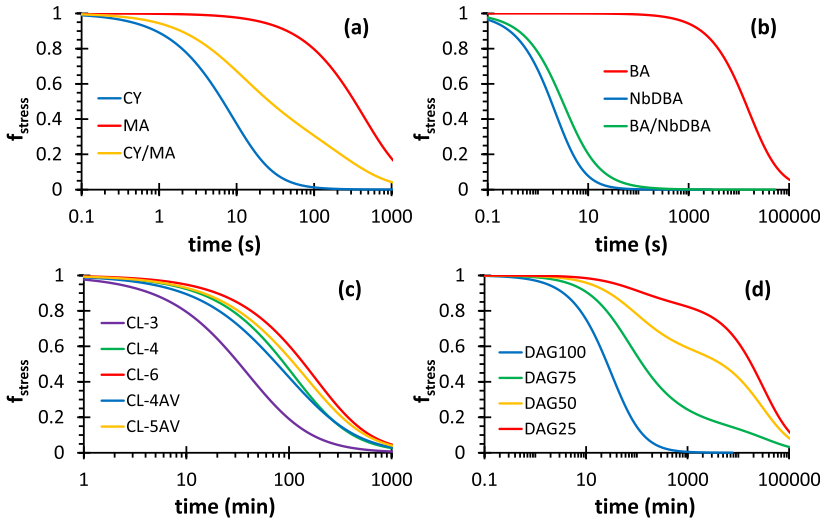

Figure 11. Simulation of complex relaxation cases reported in the literature: (a) PDMS crosslinked with Meldrum acid derivatives[13] (see Figure 5a in reference), (b) PDMS diols crosslinked with boronic acids[14] (see Figures 4f and 5c in reference), (c) thiol-epoxy vitrimers with different functionality and mixtures[15] (see Figure 8 in reference), and (d) thiol−ene vitrimers with disulfide and transesterification bond exchange[12] (see Figures 1 and 3 in the reference). The same nomenclature as in the original references has been used. Details of the simulations can be found in the Supporting Information.

consideration when designing a network with mixed kinetic behavior.

Examination of the results in Figure 10 leads to the hypothesis that highly broad relaxation profiles such as those observed in thiol-epoxy vitrimers[6,15,42] may arise from the existence of multiple species with different relaxation kinetics. It is known that vitrimers based on transesterification undergo a significant network rearrangement, leading to a redistribution of structural fragments, along with the formation of new ones, within the network structure.[29,30] This is expected to occur in thiol-epoxy vitrimers as well, leading to a range of structural fragments with a complex distribution of (−) and (+) bonds that cannot be analyzed using the current methodology. A modeling effort of this particular scenario is called for, but this is out of the scope of this work.

Additional effects of monomer structure and the contribution of truly static bonds could be incorporated. As a matter of fact, the number of cases to be analyzed is endless. For the sake of brevity, we will limit further analysis to the application of this modeling methodology to a number of selected cases from the literature. Some of these cases are illustrated in Figure 11 and also in the Supporting Information.

It is widely documented that the combination of components with different relaxation kinetics can lead to intermediate mixture behavior.[13,14,47] In all these cases, predictions made using this model produce remarkably good results. For instance, the analysis of poly(dimethylsiloxane) (PDMS) rubber crosslinked with Meldrum acid derivatives with different exchange dynamics[13] in Figure 11a (see also Figure S6 in Supporting Information) produces striking similarities with the reported data, showing a broad two-step behavior for the mixed system because of the high functionality of the cross-linked rubber, making $r_{dyn1} < r_{dyn}{}^{*}$. PDMS diols crosslinked with boronic esters with different activity[14] is also satisfactorily modeled in Figure 11b (see also Figure S7 in Supporting Information). The low functionality of the components used does not lead to a broad relaxation for the mixed system, but a narrow one, much closer to the relaxation of the faster component since $r_{dyn1} > r_{dyn}{}^{*}$ and the material is able to relax completely with the participation of the fastest component only. The difference between these two cases illustrates the importance of adjusting the ratio of the different components, taking into consideration the functionality of the components in the mixture. Higher functional components, as discussed above, are more prone to present complex relaxation behavior. Mixtures of dynamic hydrogels[47] also have a predictable behavior, which is in fact very similar to the data presented in Figure 10. In all these cases, the overall crosslinking density is not affected significantly, and therefore no additional effects of network mobility are expected.

In other cases, such as thiol-epoxy vitrimers with varying thiol functionality,[15] reasonable predictions of the expected mixing behavior can be made, as seen in Figure 11c (see also Figure S8 in Supporting Information), even if the model is not able to predict accurately the value of the shape parameter β due to the structural complexity of the system. However, it is not clear whether the observed effect results from different intrinsic bond exchange dynamics or else there is an additional effect of crosslinking density on chain mobility. Other mixing effects have been reported, such as in imine vitrimers prepared from amines of different sizes and structures.[17] However, the reported trends are not correctly reproduced using a complex relaxation model, which produces an exceedingly large broadening effect (results not shown). Since there is no apparent reason for a difference in reactivity, such systems would be better reproduced using a simple relaxation model but with a mixture of components (see previous section), with the kinetic effect of the crosslinking density incorporated into the bond exchange constant.

The effect of the addition of a fast relaxing component, in a similar way to one of the systems reported by Van Lijsebetten et al., can also be modeled.[8] This scenario is similar to the relaxation curves in Figure 10, upper graph (see Figure S9 in Supporting Information for specific analysis of this case). The data can be fitted to multiple Maxwell models with a reasonable trend, especially at higher contributions of the

https://doi.org/10.1021/acs.macromol.3c00482
Macromolecules 2023, 56, 4855−4873

faster components, when the difference in adjusted relaxation times compares better with the bond exchange constants.[8] This increases accuracy in comparison to using a single Maxwell element and even to a stretched exponential (Figure S9 in Supporting Information). However, the relative contribution of the Maxwell elements in terms of the global stress relaxation is unclear (see table in Figure S9 in Supporting Information), considering that a very small amount of the fast component is added and its contribution to the relaxed stress should be minor. As discussed in the previous section, a value of $\beta < 1$ may not be indicative of kinetic complexity. The relaxation data might be fitted to multiple Maxwell elements but an interpretation in terms of the existence of complex relaxation kinetics would be inaccurate.

The results reported by Konuray et al. combining two distinct relaxation mechanisms[12] were also simulated in Figure 11d (see also Figure S10 in Supporting Information), with results showing comparable effects to the ones reported. Even if the dynamic bond exchange process is modeled somewhat differently from the real system, the quality of the simulation is remarkable. Moreover, this complex relaxation behavior is a better description of the real situation than that based on the presence of a static network (however good of an approximation it is), because no truly static bonds are present in the system. Network mobility and some non-ideal structural effects should also be considered for higher accuracy.

Therefore, it can be seen that the present modeling approach is capable of predicting the effect of combining bond exchange processes with different kinetics, considering the relative rates of bond exchange, the feed ratio of the components, and their functionalities. This makes it possible to design materials with tunable and predictable relaxation dynamics. Some additional corrections might be needed if there is additional contribution from changes in the cross-linking density or mobility of the network. A more detailed description of the structural fragments within the network would be required in order to accurately model certain systems with intrinsic structural complexity.

Dissociative CANs. The proposed model is also capable of reproducing stress relaxation processes of dissociative CANs, given their structural description and detailed kinetics information. To demonstrate, we choose to simulate the behavior of furan-maleimide Diels–Alder networks. Such networks generally show a strongly temperature-dependent equilibrium, leading to significant changes in the network structure with temperature.[31] In the recent years, Van Assche and co-workers have analyzed in detail and modeled the reaction kinetics of different CANs based on the Diels–Alder reaction.[34,35,48] Strachota et al. studied CANs with a controlled structure and gelation based on the Diels–Alder reaction and their use in self-healing applications.[31,32] Different researchers have analyzed the stress relaxation of CANs based on the Diels–Alder reaction.[26,28,49] In order to model the stress relaxation of dissociative CANs, the system described by Diaz et al.[34] will be analyzed in detail, given the availability of detailed kinetic and thermal-mechanical information, and the simplicity of the network structure (i.e., suitable for simulation using the present structural model). No stress relaxation data are available for this particular system, but the results of the simulation will be compared with the results obtained by other researchers for dissociative CANs, including those based on Diels–Alder reactions.

The system studied by Diaz et al.[34] can be assimilated to an A_4D_2 system such as the one shown in Figure 4. Because of the equilibrium between the forward and retro Diels–Alder reactions (from now on referred to as DA and retro-DA reactions, respectively), increasing the temperature leads to networks with increasing degree of dissociation, eventually leading to degelation when the equilibrium dissociation conversion reaches a value of 0.42 (see Figure 4). This is equivalent to the prediction made using the Flory–Stockmayer expression for gelation, yielding a value of 0.58, which corresponds to a degelation equilibrium temperature slightly below 90 °C for this system.[34] Adzima et al. also found a good agreement between the theoretical predictions using the Flory–Stockmayer equation and experimental results.[33]

First of all, we validated the kinetic model. For the DA reaction, we take $\ln A_{DA} = 11.7$ kg·mol^{-1}·s^{-1} and $E_{DA} = 53.9$ kJ·mol^{-1}; for the retro-DA reaction, we use $\ln A_{rDA} = 28.3$ s^{-1} and $E_{rDA} = 105.7$ kJ·mol^{-1}.[34] With these parameters and for a given temperature, we can calculate k_{DA} using the equation $k_{DA} = \exp(\ln A_{DA} - E_{DA}\cdot 1000/(R\cdot T))$ (in kg·mol^{-1}·s^{-1}). k_{rDA} (in s^{-1}) can be calculated in a similar fashion. According to the kinetics and equilibrium model described in the Theory section, $k_{back}' = k_{rDA}$ (in s^{-1}) and $k_{for}' = k_{DA}\cdot[A]_0$, where $[A]_0 = 1.8$ mol/kg is the total concentration of exchangeable bonds in the material (i.e., total concentration of furan or maleimide groups).

In Figure 12a we present the equilibrium dissociation conversion with respect to temperature, and the dissociation

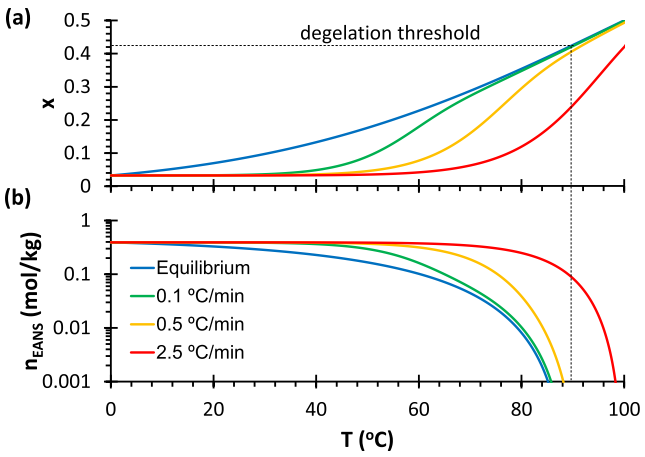

Figure 12. Prediction of the extent of dissociation (a) and the concentration of EANS (n_{EANS}) (b) during heating of a A_4D_2 CAN based on the Diels–Alder reaction reported in the literature,[34] at different heating rates in comparison with the equilibrium process. The dashed line represents the degelation threshold for dissociation conversion and temperature.

conversion at different heating rates starting from an equilibrium situation at 0 °C. The results compare well with those reported in the literature,[34] considering that we use x as bond dissociation conversion (decrosslinking process), instead of bond formation (crosslinking process). With increasing heating rates, a delay is observed in the dissociation conversion relative to the equilibrium line. At sufficiently low heating rates (i.e., 0.5 °C/min), no practical difference is observed at temperatures above 90 °C, as expected.[34]

An interesting feature of the model is the prediction of the real and effective crosslinking density given by the calculation of n_{EANS} (see eq 17) (Figure 12b) in a given heating program.

https://doi.org/10.1021/acs.macromol.3c00482
Macromolecules 2023, 56, 4855–4873

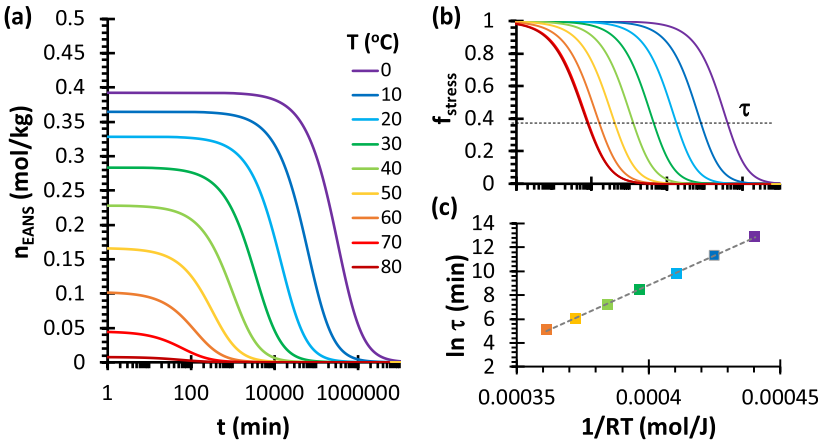

Figure 13. Simulation of the stress relaxation of the DA network described in the work of Diaz et al.[34] The main graph (a) represents the calculated crosslinking density with elastic activity, the side graph (b) represents the normalized stress relaxation [same timescale as (a)], and the side graph (c) represents the determination of the apparent activation energy of the relaxation process.

A real change in network crosslinks is taking place due to the shift of the equilibrium concentration with temperature and the kinetics of the forward and backward reactions. At 0 °C, a value of n_{EANS} = 0.39 mol/kg, corresponding to a dissociation extent x = 0.033 can be calculated. Assuming a density ρ = 1.1 kg/m^3, we can estimate an elastic modulus as $G = n_{EANS} \cdot \rho \cdot R \cdot T \simeq 1$ MPa, and $E \simeq 3 \cdot G = 3$ MPa, in excellent agreement with the data reported by Diaz et al.[34] The evolution of the equilibrium modulus also follows the same trend as reported up to moderate temperatures, with some discrepancies at higher temperatures due to the contribution of other effects.[34] Moreover, the model also predicts that, at 2.5 °C/min, n_{EANS} remains fairly constant at moderate temperatures because of the delay in the change in the concentration of bonds with respect to the equilibrium, as seen in the upper graph. Then it starts to decrease noticeably, leading to a 10-fold drop in n_{EANS} at a temperature around 93 °C. If this is compared with the data at the same heating rate, neglecting the effect of the α-relaxation of the material, a similar behavior of the storage modulus E' is observed, and the same 10-fold drop in storage modulus E' is obtained at 86−88 °C.[34] Taking into consideration that the elastic modulus is proportional to the effective crosslinking density, it can be concluded that the model can predict the evolution of the material structure with temperature.

By way of contrast, Strachota et al. analyzed crosslinking of several DA systems both experimentally and theoretically, making use of a structural model based on the theory of branching processes,[31] which is equivalent to the structural model used in this work. Their comparison between the predicted equilibrium modulus and the experimental modulus measured at a given heating rate showed non-negligible differences, which are comparable to the differences observed in the comparison of n_{EANS} under equilibrium conditions and at different heating rates shown in Figure 12b, hence the importance of having detailed kinetic information of the system.

Other researchers attempted a structural modeling in dissociative CANs and used the experimental moduli to determine the extent of dissociation.[8] In the present case, the method used the prediction of the initial modulus starting from equilibrium thermodynamics considerations and a sound structural model, yielding modulus and stress estimates with a high degree of accuracy.

A general and practical aspect of this modeling methodology concerns the requirement of equilibration of the network structure prior to the analysis of the stress relaxation or any other phenomena. This is to ensure reproducibility and to avoid misleading results. In the case of associative CANs or other networks in which the network structure has very little temperature dependence, it is sufficient to ensure thermal equilibrium is reached, which takes only a few minutes. In the case of dissociative CANs whose network structures are highly temperature-dependent, it is crucial to ensure that the forward and backward reactions have attained equilibrium. Using the kinetic data available for this system, long isothermal stabilization times can be predicted, especially at lower temperatures (see Figure S11 in Supporting Information). Nevertheless, this period could be considerably shortened by overheating and then reducing the temperature, exploiting the observed hysteresis effect in the kinetics of the reaction with respect to the equilibrium.[34]

We calculated the relaxation process starting from equilibrium at different temperatures, using the kinetic-structural model described in the Theory section. It is assumed that, once the network is in equilibrium conditions, further decrosslinking will not occur in the course of the stress relaxation process, since the rates of the forward and backward reactions are the same, producing no net change in bonded species. It must be remembered that the present modeling of the stress relaxation assumes that the concentration of bonded species is not changing during the relaxation process at constant temperature; rather, they change their configuration, leading to a decrease of crosslinks or network strands with elastic activity. It is also assumed that the rate of effective dynamic bond exchange (that is, producing an effect on the stress relaxation) is related to the rate of the dissociation (backward) reaction. In consequence, for the material of Diaz et al.,[34] one could use the retro-DA rate constant in order to model the stress relaxation, so that $k_{exch} = k_{rDA}$. It should be noted that the rate constants determined for this dissociative bond exchange process are valid within the whole range of bond association/dissociation.[34] In other words, the network and chain mobility can change substantially depending on initial equilibrium temperature, but this does not affect the

https://doi.org/10.1021/acs.macromol.3c00482
Macromolecules 2023, 56, 4855−4873

value of the association/dissociation rate constants, unlike other bond exchange processes.

The results of this simulation are shown in Figure 13a. As can be observed, there is an initial equilibrium concentration of EANS (n_{EANS}) that decreases with increasing temperature, in accordance with the data shown in Figure 12. This decreasing initial value of n_{EANS} with respect to temperature should result in a lower value of initial relaxation stress or modulus. At low temperatures, a stress relaxation process takes place at an extremely slow rate. As the temperature increases, the initial n_{EANS} or relaxation modulus decreases, but the relaxation process proceeds at a faster rate. At temperatures close to the degelation temperature, the initial modulus is extremely low. From a qualitative point of view, these simulated relaxation profiles compare well to the experimental results reported for other dissociative networks.[8,26,27] It can also be seen that the timescale of the stress relaxation experiment is comparable to that for the thermal stabilization of the sample (see Figure S11 in Supporting Information).

In order to analyze the relaxation kinetics, the stress relaxation curves are normalized to a reference value, as done by other researchers.[27,28] In fact, in Figure 13b, it is observed that all normalized curves have a similar shape (with shape factor β values between 0.97 and 0.85 using the present model). The spacing between the curves is also quite regular except for the curves at the highest temperatures, which seem to overlap. The starting point of the relaxation process changes significantly with temperature (i.e., with the extent of bond dissociation) (see Figure 12), but they reach the same state of relaxation (equivalent to a state of dissociation at $x = 0.42$) and with a highly similar profile. In fact, when the relaxation times τ are analyzed by plotting ln τ with respect to the inverse of temperature, as shown in Figure 13c, a line is obtained with a slope equal to 99.2 kJ/mol, a value similar to those reported for other CANs based on the Diels−Alder reaction[24,26,28,49] and close to the activation energy of the retro-DA reaction of 105.7 kJ/mol. The relaxation times are nearly proportional to the bond lifetime estimated as the inverse of the dissociation constant, $\tau_b \simeq 1/k_{rDA}$. Such a similarity between the activation energies of stress relaxation experiments and dissociation reactions was reported for CANs based on Diels−Alder reactions and others.[26,28] Therefore, this modeling practice confirms the experimental observation that kinetics of the stress relaxation process are governed by the rate of dissociation.[28]

CONCLUSIONS

A methodology capable of describing the kinetics of stress relaxation of CANs has been presented. The methodology is based on the analysis of the deactivation of EANS during stress relaxation, by means of a well-established recursive model originally intended for the analysis of crosslinking processes. The decrosslinking is only apparent, since network integrity is retained, with the exchange reactions simply transforming the status of the bonds in the network structure from elastically active to elastically inactive. The structural model is combined with a kinetic model describing the effective rate of disconnection of bonds during the process. Using this comprehensive framework, a wide range of simple and complex scenarios have been analyzed and the prediction capabilities of the combined model have been validated by comparison with a number of selected cases from the literature.

The results show that the architectural design of a dynamic network is a strong determinant of the relaxation kinetics. It has been shown that full stress relaxation does not require the participation of all the dynamic bonds present in the network, although the relaxation kinetics strongly depend on their presence. The use of higher functional monomers or oligomers requires further bond exchange to achieve full stress relaxation. This is due not only to slower relaxation kinetics but also to effects such as mobility restrictions. Complete relaxation and full recycling capabilities can be achieved in polymer networks despite a reduced contribution from dynamic bonds. In such cases, relaxation kinetics are hindered, but this can have a beneficial effect in terms of controlling undesired creep. With the proposed model, complex kinetic effects resulting from the combination of components with different bond exchange kinetics can be satisfactorily modeled. Another practical implication of the results is that fine-tuning the relaxation dynamics requires not only the use of components with intrinsic differences, but also a suitable material design in terms of monomer functionality and feed ratio of the components. The analysis of stress relaxation processes in dissociative CANs produces results comparable to those based on associative bond exchange, but detailed kinetic and thermodynamics information are required in order to test the time−temperature programs required for their use in practical applications.

In general, the results from the present modeling approach reveal an unprecedented flexibility in the design of materials based on CANs with a wide range of vitrimer-like capabilities suitable for a variety of reprocessing and recycling scenarios. The methodology could be improved by incorporating non-ideal effects such as incomplete reaction or intra-molecular cyclization and advanced kinetic effects depending on the network mobility or the presence of catalytic species. Given the possibility to accurately define structural fragments and given the availability of thermodynamic and kinetic data, one can study other types of polymer networks such as (a) off-stoichiometric step-wise systems with homopolymerization of the excess groups leading to permanent network structure, (b) step-wise systems with intra-molecular dynamic bond exchange, (c) materials obtained by crosslinking of polymer chains, or (d) CANs based on chain-wise polymerization processes.

ASSOCIATED CONTENT

Supporting Information

The Supporting Information is available free of charge at https://pubs.acs.org/doi/10.1021/acs.macromol.3c00482.

Detailed mathematical description and derivation of the stress relaxation model presented in the work and simulation details for the analysis of simple and complex relaxation processes and for the comparison with literature data (PDF)

AUTHOR INFORMATION

Corresponding Author

Xavier Fernández-Francos − *Thermodynamics Laboratory ETSEIB, Universitat Politècnica de Catalunya, 08028 Barcelona, Spain;* orcid.org/0000-0002-3492-2922; Phone: +34 934017955; Email: xavier.fernandez@upc.edu

https://doi.org/10.1021/acs.macromol.3c00482
Macromolecules 2023, 56, 4855−4873

Authors

Osman Konuray − *Thermodynamics Laboratory ETSEIB, Universitat Politècnica de Catalunya, 08028 Barcelona, Spain;* orcid.org/0000-0001-7281-006X

Xavier Ramis − *Thermodynamics Laboratory ETSEIB, Universitat Politècnica de Catalunya, 08028 Barcelona, Spain;* orcid.org/0000-0003-2550-7185

Complete contact information is available at: https://pubs.acs.org/10.1021/acs.macromol.3c00482

Notes

The authors declare no competing financial interest.

■ ACKNOWLEDGMENTS

This work was funded by the Spanish Ministry of Science and Innovation (MCIN/AEI/10.13039/501100011033) through R&D project PID2020-115102RB-C22 and also by Generalitat de Catalunya (2017-SGR-77). X. Fernández-Francos and O. Konuray acknowledge the Serra-Húnter programme (Generalitat de Catalunya).

■ REFERENCES

(1) Alabiso, W.; Schlögl, S. The Impact of Vitrimers on the Industry of the Future: Chemistry, Properties and Sustainable Forward-Looking Applications. *Polymers* **2020**, *12*, 1660.

(2) Kloxin, C. J.; Scott, T. F.; Adzima, B. J.; Bowman, C. N. Covalent Adaptable Networks (CANs): A Unique Paradigm in Cross-Linked Polymers. *Macromolecules* **2010**, *43*, 2643−2653.

(3) Denissen, W.; Winne, J. M.; Du Prez, F. E. Vitrimers: Permanent Organic Networks with Glass-like Fluidity. *Chem. Sci.* **2016**, *7*, 30−38.

(4) Cuminet, F.; Caillol, S.; Dantras, É.; Leclerc, É.; Ladmiral, V. Neighboring Group Participation and Internal Catalysis Effects on Exchangeable Covalent Bonds: Application to the Thriving Field of Vitrimer Chemistry. *Macromolecules* **2021**, *54*, 3927−3961.

(5) Winne, J. M.; Leibler, L.; Du Prez, F. E. Dynamic Covalent Chemistry in Polymer Networks: A Mechanistic Perspective. *Polym. Chem.* **2019**, *10*, 6091−6108.

(6) Li, L.; Chen, X.; Jin, K.; Torkelson, J. M. Vitrimers Designed Both To Strongly Suppress Creep and To Recover Original Cross-Link Density after Reprocessing: Quantitative Theory and Experiments. *Macromolecules* **2018**, *51*, 5537−5546.

(7) Breuillac, A.; Kassalias, A.; Nicolaÿ, R. Polybutadiene Vitrimers Based on Dioxaborolane Chemistry and Dual Networks with Static and Dynamic Cross-Links. *Macromolecules* **2019**, *52*, 7102−7113.

(8) Van Lijsebetten, F.; De Bruycker, K.; Van Ruymbeke, E.; Winne, J. M.; Du Prez, F. E. Characterising Different Molecular Landscapes in Dynamic Covalent Networks. *Chem. Sci.* **2022**, *13*, 12865−12875.

(9) Xiang, S.; Zhou, L.; Chen, R.; Zhang, K.; Chen, M. Interlocked Covalent Adaptable Networks and Composites Relying on Parallel Connection of Aromatic Disulfide and Aromatic Imine Cross-Links in Epoxy. *Macromolecules* **2022**, *55*, 10276−10284.

(10) Wang, L.; Liu, Y.; Qiao, Y.; Wang, Y.; Cui, Z.; Zhu, S.; Dong, F.; Fang, S.; Du, A. Molecularly Engineered Dual-Crosslinked Elastomer Vitrimers with Superior Strength, Improved Creep Resistance, and Retained Malleability. *Polym. Chem.* **2022**, *13*, 4144−4153.

(11) Van Lijsebetten, F.; De Bruycker, K.; Spiesschaert, Y.; Winne, J. M.; Du Prez, F. E. Suppressing Creep and Promoting Fast Reprocessing of Vitrimers with Reversibly Trapped Amines. *Angew. Chem., Int. Ed.* **2022**, *61*, No. e202113872.

(12) Konuray, O.; Moradi, S.; Roig, A.; Fernández-Francos, X.; Ramis, X. Thiol−Ene Networks with Tunable Dynamicity for Covalent Adaptation. *ACS Appl. Polym. Mater.* **2023**, *5*, 1651−1656.

(13) El-Zaatari, B. M.; Ishibashi, J. S. A.; Kalow, J. A. Cross-Linker Control of Vitrimer Flow. *Polym. Chem.* **2020**, *11*, 5339−5345.

(14) Porath, L.; Huang, J.; Ramlawi, N.; Derkaloustian, M.; Ewoldt, R. H.; Evans, C. M. Relaxation of Vitrimers with Kinetically Distinct Mixed Dynamic Bonds. *Macromolecules* **2022**, *55*, 4450−4458.

(15) Isogai, T.; Hayashi, M. Critical Effects of Branch Numbers at the Cross-Link Point on the Relaxation Behaviors of Trans-esterification Vitrimers. *Macromolecules* **2022**, *55*, 6661−6670.

(16) Melchor Bañales, A. J.; Larsen, M. B. Thermal Guanidine Metathesis for Covalent Adaptable Networks. *ACS Macro Lett.* **2020**, *9*, 937−943.

(17) Hajj, R.; Duval, A.; Dhers, S.; Avérous, L. Network Design to Control Polyimine Vitrimer Properties: Physical Versus Chemical Approach. *Macromolecules* **2020**, *53*, 3796−3805.

(18) Zhao, S.; Abu-Omar, M. M. Catechol-Mediated Glycidylation toward Epoxy Vitrimers/Polymers with Tunable Properties. *Macromolecules* **2019**, *52*, 3646−3654.

(19) Hayashi, M.; Yano, R. Fair Investigation of Cross-Link Density Effects on the Bond-Exchange Properties for Trans-Esterification-Based Vitrimers with Identical Concentrations of Reactive Groups. *Macromolecules* **2020**, *53*, 182−189.

(20) Chen, M.; Si, H.; Zhang, H.; Zhou, L.; Wu, Y.; Song, L.; Kang, M.; Zhao, X.-L. The Crucial Role in Controlling the Dynamic Properties of Polyester-Based Epoxy Vitrimers: The Density of Exchangeable Ester Bonds (υ). *Macromolecules* **2021**, *54*, 10110−10117.

(21) Hu, S.; Chen, X.; Torkelson, J. M. Biobased Reprocessable Polyhydroxyurethane Networks: Full Recovery of Crosslink Density with Three Concurrent Dynamic Chemistries. *ACS Sustainable Chem. Eng.* **2019**, *7*, 10025−10034.

(22) Wu, S.; Yang, H.; Xu, W.-S.; Chen, Q. Thermodynamics and Reaction Kinetics of Symmetric Vitrimers Based on Dioxaborolane Metathesis. *Macromolecules* **2021**, *54*, 6799−6809.

(23) Wu, S.; Yang, H.; Huang, S.; Chen, Q. Relationship between Reaction Kinetics and Chain Dynamics of Vitrimers Based on Dioxaborolane Metathesis. *Macromolecules* **2020**, *53*, 1180−1190.

(24) Elling, B. R.; Dichtel, W. R. Reprocessable Cross-Linked Polymer Networks: Are Associative Exchange Mechanisms Desirable? *ACS Cent. Sci.* **2020**, *6*, 1488−1496.

(25) Scheutz, G. M.; Lessard, J. J.; Sims, M. B.; Sumerlin, B. S. Adaptable Crosslinks in Polymeric Materials: Resolving the Intersection of Thermoplastics and Thermosets. *J. Am. Chem. Soc.* **2019**, *141*, 16181−16196.

(26) Chakma, P.; Morley, C. N.; Sparks, J. L.; Konkolewicz, D. Exploring How Vitrimer-like Properties Can Be Achieved from Dissociative Exchange in Anilinium Salts. *Macromolecules* **2020**, *53*, 1233−1244.

(27) Jourdain, A.; Asbai, R.; Anaya, O.; Chehimi, M. M.; Drockenmuller, E.; Montarnal, D. Rheological Properties of Covalent Adaptable Networks with 1,2,3-Triazolium Cross-Links: The Missing Link between Vitrimers and Dissociative Networks. *Macromolecules* **2020**, *53*, 1884−1900.

(28) Kuang, X.; Liu, G.; Dong, X.; Wang, D. Correlation between Stress Relaxation Dynamics and Thermochemistry for Covalent Adaptive Networks Polymers. *Mater. Chem. Front.* **2017**, *1*, 111−118.

(29) Altuna, F. I.; Hoppe, C. E.; Williams, R. J. Epoxy Vitrimers: The Effect of Transesterification Reactions on the Network Structure. *Polymers* **2018**, *10*, 43.

(30) Altuna, F. I.; Hoppe, C. E.; Williams, R. J. J. Epoxy Vitrimers with a Covalently Bonded Tertiary Amine as Catalyst of the Transesterification Reaction. *Eur. Polym. J.* **2019**, *113*, 297−304.

(31) Strachota, B.; Morand, A.; Dybal, J.; Matějka, L. Control of Gelation and Properties of Reversible Diels−Alder Networks: Design of a Self-Healing Network. *Polymers* **2019**, *11*, 930.

(32) Strachota, B.; Hodan, J.; Dybal, J.; Matějka, L. Self-Healing Epoxy and Reversible Diels-Alder Based Interpenetrating Networks. *Macromol. Mater. Eng.* **2021**, *306*, 2000474.

(33) Adzima, B. J.; Aguirre, H. A.; Kloxin, C. J.; Scott, T. F.; Bowman, C. N. Rheological and Chemical Analysis of Reverse Gelation in a Covalently Cross-Linked Diels−Alder Polymer Network. *Macromolecules* **2008**, *41*, 9112−9117.

(34) Diaz, M. M.; Van Assche, G.; Maurer, F. H. J.; Van Mele, B. Thermophysical Characterization of a Reversible Dynamic Polymer Network Based on Kinetics and Equilibrium of an Amorphous Furan-Maleimide Diels-Alder Cycloaddition. *Polymer* **2017**, *120*, 176−188.
(35) Mangialetto, J.; Verhelle, R.; Van Assche, G.; Van den Brande, N.; Van Mele, B. Time-Temperature-Transformation, Temperature-Conversion-Transformation, and Continuous-Heating-Transformation Diagrams of Reversible Covalent Polymer Networks. *Macromolecules* **2021**, *54*, 412−425.
(36) Parada, G. A.; Zhao, X. Ideal Reversible Polymer Networks. *Soft Matter* **2018**, *14*, 5186−5196.
(37) Pascault, J.-P. P.; Sautereau, H.; Verdu, J.; Williams, R. J. J. *Thermosetting Polymers*; Marcel Dekker: New York, 2002.
(38) Miller, D. R.; Macosko, C. W. A New Derivation of Post Gel Properties of Network Polymers. *Macromolecules* **1976**, *9*, 206−211.
(39) Miller, D. R.; Valles, E. M.; Macosko, C. W. Calculation of Molecular Parameters for Stepwise Polyfunctional Polymerization. *Polym. Eng. Sci.* **1979**, *19*, 272−283.
(40) Lesser, A. J.; Crawford, E. The Role of Network Architecture on the Glass Transition Temperature of Epoxy Resins. *J. Appl. Polym. Sci.* **1997**, *66*, 387−395.
(41) Charlesworth, J. M. Effect of Crosslink Density on Molecular Relaxations in Diepoxide-Diamine Network Polymers. Part 2. The Rubbery Plateau Region. *Polym. Eng. Sci.* **1988**, *28*, 230−236.
(42) Hayashi, M.; Katayama, A. Preparation of Colorless, Highly Transparent, Epoxy-Based Vitrimers by the Thiol-Epoxy Click Reaction and Evaluation of Their Shape-Memory Properties. *ACS Appl. Polym. Mater.* **2020**, *2*, 2452−2457.
(43) Li, L.; Chen, X.; Torkelson, J. M. Reprocessable Polymer Networks via Thiourethane Dynamic Chemistry: Recovery of Cross-Link Density after Recycling and Proof-of-Principle Solvolysis Leading to Monomer Recovery. *Macromolecules* **2019**, *52*, 8207−8216.
(44) Casado, J.; Konuray, O.; Benet, G.; Fernández-Francos, X.; Morancho, J. M.; Ramis, X. Optimization and Testing of Hybrid 3D Printing Vitrimer Resins. *Polymers* **2022**, *14*, 5102.
(45) Casado, J.; Konuray, O.; Roig, A.; Fernández-Francos, X.; Ramis, X. 3D Printable Hybrid Acrylate-Epoxy Dynamic Networks. *Eur. Polym. J.* **2022**, *173*, 111256.
(46) Chen, M.; Zhou, L.; Wu, Y.; Zhao, X.; Zhang, Y. Rapid Stress Relaxation and Moderate Temperature of Malleability Enabled by the Synergy of Disulfide Metathesis and Carboxylate Transesterification in Epoxy Vitrimers. *ACS Macro Lett.* **2019**, *8*, 255−260.
(47) Yesilyurt, V.; Ayoob, A. M.; Appel, E. A.; Borenstein, J. T.; Langer, R.; Anderson, D. G. Mixed Reversible Covalent Crosslink Kinetics Enable Precise, Hierarchical Mechanical Tuning of Hydrogel Networks. *Adv. Mater.* **2017**, *29*, 1605947.
(48) Cuvellier, A.; Verhelle, R.; Brancart, J.; Vanderborght, B.; Van Assche, G.; Rahier, H. The Influence of Stereochemistry on the Reactivity of the Diels−Alder Cycloaddition and the Implications for Reversible Network Polymerization. *Polym. Chem.* **2019**, *10*, 473−485.
(49) Wei, Z.; Wang, Y.; Fu, X.; Jiang, L.; Wang, Y.; Yuan, A.; Xu, H.; Lei, J. Recyclable and Reprocessable Thermosetting Polyurea with High Performance Based on Diels-Alder Dynamic Covalent Cross-linking. *Macromol. Res.* **2021**, *29*, 562−568.

https://doi.org/10.1021/acs.macromol.3c00482
Macromolecules 2023, 56, 4855−4873